
Contrastive and Non-Contrastive Self-Supervised Learning Recover Global and Local Spectral Embedding Methods

Randall Balestriero
Meta AI Research
NYC, USA
rbalestriero@fb.com

Yann LeCun
Meta AI Research & NYU
NYC, USA
ylecun@fb.com

Abstract

Self-Supervised Learning (SSL) surmises that inputs and pairwise positive relationships are enough to learn meaningful representations. Although SSL has recently reached a milestone: outperforming supervised methods in many modalities... the theoretical foundations are limited, method-specific, and fail to provide principled design guidelines to practitioners. In this paper, we propose a unifying framework under the helm of spectral manifold learning to address those limitations. Through the course of this study, we will rigorously demonstrate that VICReg, SimCLR, BarlowTwins et al. correspond to eponymous spectral methods such as Laplacian Eigenmaps, Multidimensional Scaling et al. This unification will then allow us to obtain (i) the closed-form optimal representation for each method, (ii) the closed-form optimal network parameters in the linear regime for each method, (iii) the impact of the pairwise relations used during training on each of those quantities and on downstream task performances, and most importantly, (iv) the first theoretical bridge between contrastive and non-contrastive methods towards global and local spectral embedding methods respectively, hinting at the benefits and limitations of each. For example, (i) if the pairwise relation is aligned with the downstream task, any SSL method can be employed successfully and will recover the supervised method, but in the low data regime, VICReg’s invariance hyper-parameter should be high; (ii) if the pairwise relation is misaligned with the downstream task, VICReg with small invariance hyper-parameter should be preferred over SimCLR or BarlowTwins.

1 Introduction

Self-Supervised Learning (SSL) is one of the most promising method to learn data representations that generalize across downstream tasks. SSL places itself in-between supervised and unsupervised learning as it does not require labels but does require knowledge of what makes some samples semantically close to others. Hence, where unsupervised learning relies on a collection of inputs (\mathbf{X}), and supervised learning relies on inputs and outputs (\mathbf{X}, \mathbf{Y}), SSL relies on inputs and inter-sample relations (\mathbf{X}, \mathbf{G}) that indicate semantic similarity akin to weak-supervision used in metric learning [Xing et al., 2002]. The latter matrix \mathbf{G} is often constructed by augmenting \mathbf{X} through data-augmentations known to preserve input semantics [Kanazawa et al., 2016, Novotny et al., 2018, Gidaris et al., 2018] e.g. horizontal flip for an image, although recent methods have went away from DA by using videos from which consecutive frames can be seen as semantically equivalent [Sermanet et al., 2018, Kim et al., 2019, Xu et al., 2019].

Although SSL originated decades ago [Bromley et al., 1993], recent advances have pushed SSL performances beyond expectations [Chen et al., 2020, Misra and Maaten, 2020, Caron et al., 2021]. Due to those rapid empirical advances, an urgent need for a principled theoretical understanding of those methods has emerged

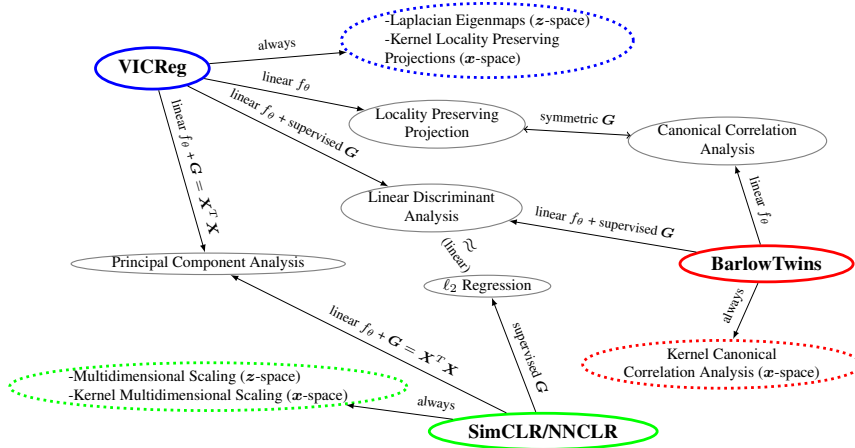


Figure 1: Summary of our unification of SSL methods to known *local* and *global* spectral embedding methods. In doing so, we are able to find the exact settings for which different methods provably become identical. In short, all are concerned in preserving the left-singular vectors of the similarity matrix G (see Fig. 3) in the representation Z .

e.g. to understand how well the learned transformation transfer to different downstream tasks [Goyal et al., 2019, Ericsson et al., 2021]. Studies looking to provide a more fundamental and principled understanding of SSL mostly take one of the three following approaches: (i) studying the training dynamics and optimization landscapes in a linear network regime e.g. validating some empirically found tricks as necessary conditions for stable gradient dynamics Wang et al. [2021], Tian et al. [2021], Wen and Li [2021], Pokle et al. [2022], Tian [2022], (ii) studying the role of individual SSL components separately e.g. the projector and predictor networks Hua et al. [2021], Jing et al. [2021], Bordes et al. [2021], Tosh et al. [2021], or (iii) developing novel SSL criteria that often combine multiple interpretable objectives that a SSL model must fulfill [Arora et al., 2019, Nazi et al., 2019, Wang and Isola, 2020, Shi et al., 2020, Zbontar et al., 2021, Bardes et al., 2021]. While those branches have led to novel understandings and even stem novel SSL methods, some fundamental questions remain open.

More recently and particularly relevant to our study, Qiu et al. [2018] unified skip-gram/word2vec methods under the helm of matrix factorization. Without much effort, those results could be used to unify pretext-task SSL learning [Baevski et al., 2020, Bao et al., 2021b, He et al., 2021] (our focus is on joint-embedding SSL). Closer to our topic, HaoChen et al. [2021, 2022] developed a study of SimCLR [Chen et al., 2020] by proposing a modified objective coined as Spectral Contrastive Loss based on graph representation of pairwise similarities. A perhaps more direct connection between video-based SSL and spectral methods (Laplacian Eigenmap in particular) can be found by combining the Spectral Inference Networks (SIN) of Pfau et al. [2019] that generalize Slow Feature Analysis (SFA) to arbitrary linear operators, and the known relationship between SFA and Laplacian Eigenmap [Sprekeler, 2011]. Although SIN was not framed within an SSL viewpoint e.g. SIN has a well-posed learned coordinate system while SSL methods coordinates can be arbitrarily rotated; those studies paved our way forward as we *propose in this paper a broad analysis that unify most existing SSL methods as variants of known spectral embedding methods, allowing us for the first time to provide provable design guidelines to practitioners in their choice of architecture and methods*. We summarize our unification results in Fig. 1. The instrumental results we obtain allow us to answer some long-standing questions such as:

Are the numerous flavors of SSL methods e.g. contrastive and non-contrastive learning different representations? We demonstrate through this study that all SSL methods’ optimal learn a representation Z whose top left singular vectors align with the ones of G , and that none of the SSL methods constrain the right-singular vectors of Z .

Can we guarantee that minimizing a SSL loss produces a representation that is optimal to solve a downstream task? Yes, Section 6.3 demonstrates that a representation learned from (X, G) with any SSL loss is guaranteed to solve any downstream task (X, Y) as long as the left spectrum of G and Y are aligned.

Are there fundamental differences between contrastive and non-contrastive methods e.g. when G is unknown? We demonstrate that the optimal VICReg representation can be made full-rank while learning from G by carefully selecting the loss hyperparameters (Theorem 1 and Fig. 5), while SimCLR and BarlowTwins strictly enforce $\text{rank}(Z) = \text{rank}(G)$ (Figs. 8 and 9 respectively), hinting at a possible advantage of VICReg when G is misspecified (Section 6.4).

How does connecting SSL methods to spectral embedding methods improve our understanding and guide the design of novel SSL frameworks? We demonstrate that contrastive and non-contrastive SSL corresponds

to global and local spectral embedding methods respectively (Sections 3.2 and 4.3). From that, we easily identify the best use-cases for each of them e.g. contrastive methods aim to be metric preserving and shine with low-dimensional or high-dimensional but linear manifolds while non-contrastive shine with locally linear but globally nonlinear manifolds.

The natural symbiosis between SSL and spectral methods formulations that will be discovered throughout this study not only enables us to answer the above challenging questions but also provides practical guidelines to practitioners. One emblematic example is offered in Sections 3.3 and 5.2 where we obtain the analytical network parameters of SSL methods in the linear regime; another example is offered in Section 4.3 where novel and interpretable variations of SimCLR are obtained from first principles; or even in Section 6.4 where we identify the situations for which different SSL methods should be preferred.

We summarize our contributions below:

1. **Closed-form optimal representation for SSL losses.** The DN representation Z of inputs X learned by minimizing *any* SSL loss given a sample relation matrix G is obtained in closed-form, shedding light to many spectral properties of those representation e.g. SSL only constrains the left singular vectors and singular values of Z to align with the ones of G (Sections 3.1, 4.1 and 5.1 for VICReg, SimCLR and BarlowTwins).
2. **Closed-form optimal network parameters for SSL losses with linear networks.** The linear representation $Z = XW + b$ parameters obtained by minimizing *any* SSL loss given a sample relation matrix G are obtained in closed-form, providing insights into the type of input statistics that a network parameters focus on to produce the optimal input representation (Sections 3.3 and 5.2 for VICReg and BarlowTwins).
3. **Exact equivalence between SSL and spectral embedding methods.** SSL methods employ diverse criterion that can be tied to eponymous spectral analysis methods both when employing a nonlinear DN as Laplacian Eigenmaps (VICReg, Section 3.2), ISOMAP (SimCLR/NNCLR, Section 4.3), Canonical Correlation Analysis (BarlowTwins, Section 5.2) and when employing a linear network as Locality Preserving Projection (VICReg, Section 3.3), Canonical Correlation Analysis (BarlowTwins, Section 5.2), and Linear Discriminant Analysis for both VICReg and BarlowTwins.
4. **Optimality conditions of SSL representations on downstream tasks (Y).** When the correct data relation matrix is given i.e. with left singular vector associated to nonzero singular values that span the space of left singular vectors of the target matrix, then perfect minimization of any of those SSL losses will provide an optimal representation (Section 6.3) which —up to a rotation of its right singular vectors— is identical to the one learned in a supervised setting (Section 6.1) a necessary and sufficient condition to perfectly solve a task at hand with a linear probe (Section 6.2).

We carefully prove each statement of this study in Appendix A. To ensure clarity of our statements and results, we also provide code excerpts throughout the manuscript.

2 Notations and Background on Self-Supervised Learning

We provide in this section a brief reminder of the main Self-Supervised Learning (SSL) methods, their associated losses, and the common notations that we will rely on for the remaining of the study.

Dataset, Embedding and Relation Matrix Notations. Regardless of the loss and method employed, SSL relies on having access to a set of observations i.e. input samples $X \triangleq [\mathbf{x}_1, \dots, \mathbf{x}_N]^T \in \mathbb{R}^{N \times D}$ and a known pairwise positive relation between those samples e.g. in the form of a *symmetric* matrix $G \in \{0, 1\}^{N \times N}$ where $(G)_{i,j} = 1$ iff samples \mathbf{x}_i and \mathbf{x}_j are known to be semantically related, and with 0 in the diagonal. Commonly, one is only given a dataset $X' \in \mathbb{R}^{N' \times D'}$ where commonly $D = D'$, and artificially constructs X, G from augmentations of X' e.g. rotated, noisy versions of the original samples and turning the corresponding entries of G to be positive for the samples that have been augmented from the same original sample. The positive samples are often denoted as *views*, and in the situation where only X' is given, X is often formed as

$$X = [\text{View}_1(X')^T, \dots, \text{View}_V(X')^T]^T, \quad (1)$$

where a row $(\text{View}_v(X'))_{n,\cdot}$ is viewed as similar to the same row of $(\text{View}_{v'}(X'))_{n,\cdot}, \forall v \neq v'$. Commonly, one employs $V = 2$ i.e. only positive *pairs* are used. If one desires to duplicate a sample multiple times to obtain multiple positive pairs from the same original sample \mathbf{x}'_n , it is done by duplicating that sample within X' prior applying Eq. (1). The $\text{View}_c(\cdot), c = 1, \dots, C$ operator is a sample-wise transformation e.g. adding

white noise, masking, and the likes i.e. the same row of different view-matrix are different transformations of the same original sample from \mathbf{X}' . In the case of Eq. (1), \mathbf{G} —which will be of shape $(VN' \times VN')$ — can be easily formed via

```

1 G = torch.zeros(Np * V, Np * V) #  $\mathbf{X}' \in \mathbb{R}^{N' \times D'}$ , V is the number of views
2 i = torch.arange(0, Np * V).repeat_interleave(V - 1) # row indices
3 j = (i + torch.arange(1, V).repeat(Np * V) * Np).remainder(Np * V) # column indices
4 G[i, j] = 1 # unweighted graph connecting the rows of  $\text{View}_1(\mathbf{X}')$ , ...,  $\text{View}_V(\mathbf{X}')$ 

```

where a sparse matrix could be used for \mathbf{G} to improve efficiency, examples are provided in Fig. 3.

Lastly, we will also denote by $\mathbf{Z} \in \mathbb{R}^{N \times K}$ the matrix of feature maps or *embeddings* obtained from a model f_θ —commonly a Deep Network— such as $\mathbf{Z} \triangleq [f_\theta(\mathbf{x}_1), \dots, f_\theta(\mathbf{x}_N)]^T$

VICReg. With the above notations out of the way, we can introduce the *VICReg* loss Bardes et al. [2021] which is a function of \mathbf{X} and \mathbf{G} —although \mathbf{G} was not explicitly employed originally— as

$$\mathcal{L}_{\text{vic}} = \alpha \sum_{k=1}^K \max\left(0, 1 - \sqrt{\text{Cov}(\mathbf{Z})_{k,k}}\right) + \beta \sum_{j=1, j \neq k}^K \text{Cov}(\mathbf{Z})_{k,j}^2 + \frac{\gamma}{N} \sum_{i=1}^N \sum_{j=1}^N (\mathbf{G})_{i,j} \|\mathbf{z}_{i,\cdot} - \mathbf{z}_{j,\cdot}\|_2^2. \quad (2)$$

The VICReg loss has a computational complexity of $\mathcal{O}(NK^2 + PNK)$ with P the average number of positive samples i.e. number of nonzeros elements in each row of \mathbf{G} . Since P is often small ($P \ll K$), the computational cost is dominated by the covariance matrix, $\mathcal{O}(NK^2)$. The implementation of Eq. (2) is straightforward (details in the proof of Theorem 1) as

```

1 C = torch.cov(Z.t()) #  $\mathbf{Z} \in \mathbb{R}^{N \times K}$ 
2 var_loss = K - torch.diag(C).clamp(eps, 1).sqrt().sum() #  $\epsilon$  avoids inf. sqrt gradient at 0
3 i, j = G.nonzero(as_tuple=True) # with G as in Fig. 3, i and j are vectors of indices
4 inv_loss = (Z[i]-Z[j]).square().sum(1).inner(G[i, j])/N # pairwise  $\ell_2$  weighted by  $\mathbf{G}_{i,j}$ 
5 cov_loss = 2 * torch.triu(C, diagonal=1).square().sum() # 2x upper triangular part
6 loss = alpha * var_loss + beta * cov_loss + gamma * inv_loss # equals to (2) with  $\alpha, \beta, \gamma$ 

```

SimCLR. The SimCLR loss [Chen et al., 2020] consists in two steps. First, it produces an estimate $\hat{\mathbf{G}}(\mathbf{Z})$ of the relation matrix \mathbf{G} from the embeddings \mathbf{Z} , generally by using the cosine similarity (CoSim) as in

$$(\hat{\mathbf{G}}(\mathbf{Z}))_{i,j} = \frac{e^{\text{CoSim}(\mathbf{z}_i, \mathbf{z}_j)/\tau}}{\sum_{k=1, k \neq i}^N e^{\text{CoSim}(\mathbf{z}_i, \mathbf{z}_k)/\tau}} \mathbf{1}_{\{i=j\}}, \quad (3)$$

with $\tau > 0$ a temperature parameter. Notice that $\hat{\mathbf{G}}(\mathbf{Z})$ is a right-stochastic matrix i.e. $\hat{\mathbf{G}}(\mathbf{Z})\mathbf{1} = \mathbf{1}$. Then, SimCLR encourages the elements of $\hat{\mathbf{G}}(\mathbf{Z})$ and \mathbf{G} to match. The most popular solution to achieve that is to leverage the infoNCE loss given by

$$\mathcal{L}_{\text{simCLR}} = - \underbrace{\sum_{i=1}^N \sum_{j=1}^N (\mathbf{G})_{i,j} \log(\hat{\mathbf{G}}(\mathbf{Z}))_{i,j}}_{\text{cross-entropy between matrices}}, \quad (4)$$

where \mathbf{G} is assumed to be a right-stochastic matrix as well. If not, a simple renormalization can be applied before employing the infoNCE loss. The only difference between SimCLR and its variants e.g. NNCLR [Dwibedi et al., 2021] lies in the construction of \mathbf{G} when only given \mathbf{X}' (the input samples without any augmentation applied, recall the beginning of Section 2). As opposed to VICReg, the SimCLR loss has computational complexity of $\mathcal{O}(N^2)$ as it requires to compute all the pairwise similarities in Eq. (3). Nevertheless, Eq. (4) can be easily computed as follows (here using the CoSim again)

```

1 Z_renorm = torch.nn.functional.normalize(Z, dim=1) #  $\mathbf{Z} \in \mathbb{R}^{N \times K}$ 
2 cosim = Z_renorm @ Z_renorm.t() / tau # N x N matrix, tau is the temperature  $\tau$  from (3)
3 off_diag = cosim[~I.bool()].reshape(N, N-1) # for denom. of (3), I = torch.eye(N, N)
4 loss = (G * (torch.logsumexp(off_diag, dim=1, keepdim=True) - cosim)).sum() # gives (4)

```

BarlowTwins. Lastly, *BarlowTwins* [Zbontar et al., 2021] proposes yet a slightly different approach based on observing two views of a dataset \mathbf{X}' denoted as $\mathbf{X}'_{\text{left}}$ and $\mathbf{X}'_{\text{right}}$ and with corresponding embeddings \mathbf{Z}_{left} and $\mathbf{Z}_{\text{right}}$. The same row of those left/right matrices are the positive pairs. Denoting by \mathbf{C} the $K \times K$ cross-correlation matrix between \mathbf{Z}_{left} and $\mathbf{Z}_{\text{right}}$, we obtain the loss

$$\mathcal{L}_{\text{BT}} = \sum_{k=1}^K ((\mathbf{C})_{k,k} - 1)^2 + \alpha \sum_{k' \neq k} (\mathbf{C})_{k,k'}^2, \quad \alpha > 0. \quad (5)$$

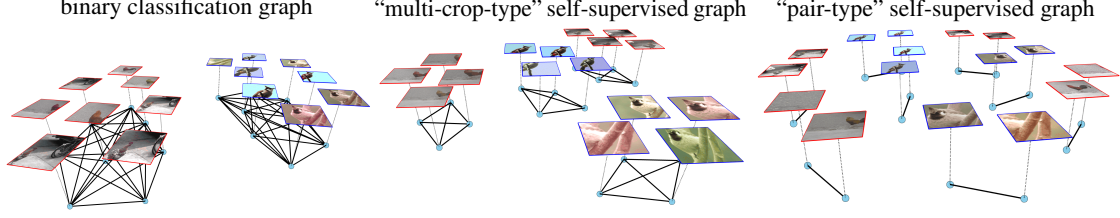


Figure 2: Depiction of the “knowledge graph” arising from different settings: binary classification (**left**), SSL with multi-crop-style relation i.e. that number of positive samples associated to each datum can be made arbitrarily large (**middle**), and pair-style SSL where each sample is only associated to another single sample (**right**). In this representation, each point can be equivalently seen as an abstract node (**blue circle**) or as a single signal $\mathbf{x}_n, n = 1, \dots, N$ (image in this case, **depicted on top**). In this case, the underlying data comes from two classes depicted with red and blue image borders. A model’s prediction on those signals $f_\theta(\mathbf{x}_n)$ can be viewed as a signal on the graph (recall Section 2). That graph is itself encoded as a symmetric, nonnegative matrix similarity matrix \mathbf{G} , as depicted in Fig. 3.

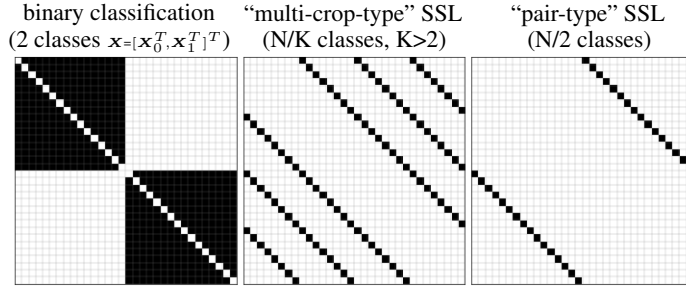


Figure 3: Examples of the $N \times N$ symmetric adjacency matrices \mathbf{G} for the three cases of Fig. 2. In all cases, each nonzero entry $(\mathbf{G})_{i,j}$ represents the positive relation between sample i and j . The insight that will play a key role in our analysis is that the eigenvectors of those matrices entirely encode the similarity information between samples that SSL utilize to constrain the learned representation (\mathbf{Z}) ’s spectrum (see Theorems 1, 5 and 6). Although \mathbf{G} is commonly symmetric, it is often not required (see Theorem 7).

Notice that $(\mathbf{C})_{i,j}$ falls back to measuring the cosine similarity between the i^{th} column of \mathbf{Z}_{left} and the j^{th} column of $\mathbf{Z}_{\text{right}}$ i.e. $(\mathbf{C})_{i,j} = \frac{\langle (\mathbf{Z}_{\text{left}})_{:,i}, (\mathbf{Z}_{\text{right}})_{:,j} \rangle}{\|(\mathbf{Z}_{\text{left}})_{:,i}\|_2 \|(\mathbf{Z}_{\text{right}})_{:,j}\|_2 + \epsilon}$ where one commonly adds an additional constant ϵ for numerical stability. The computational complexity of Eq. (5) falls back to $\mathcal{O}(NK^2)$ and its computation is easily performed as

```

1 Z_lrenorm = torch.nn.functional.normalize(Z_left, dim=0, eps=eps) # includes  $\epsilon$ 
2 Z_rrenorm = torch.nn.functional.normalize(Z_right, dim=0, eps=eps) # includes  $\epsilon$ 
3 C = Z_lrenorm.t() @ Z_rrenorm # cross-correlation (K x K matrix)
4 loss = (C.diag() - 1).square().sum() + alpha*C[~I.bool()].square().sum() # gives Eq. (5)

```

Note that if one possesses a dataset with arbitrary number of positive samples, it is still possible to recover $\mathbf{X}_{\text{left}}, \mathbf{X}_{\text{right}}$ for \mathcal{L}_{BT} with the following simple strategy. Suppose that we have 5 samples $\mathbf{a}, \mathbf{b}, \mathbf{c}, \mathbf{d}, \mathbf{e}$, and that $\mathbf{a}, \mathbf{b}, \mathbf{c}$ are related to each other, and that \mathbf{d}, \mathbf{e} are related to each other, based on \mathbf{G} . Then, one can simply create the two data matrices as

$$\mathbf{X}_{\text{left}} = [\mathbf{a}, \mathbf{a}, \mathbf{b}, \mathbf{b}, \mathbf{c}, \mathbf{c}, \mathbf{d}, \mathbf{e}]^T, \quad \mathbf{X}_{\text{right}} = [\mathbf{b}, \mathbf{c}, \mathbf{a}, \mathbf{c}, \mathbf{a}, \mathbf{b}, \mathbf{e}, \mathbf{d}]^T, \quad (6)$$

which can be easily obtained given \mathbf{G} and the input matrix \mathbf{X} via

```

1 row_indices, col_indices = G.nonzero(as_tuple=True) # G as in Fig. 3
2 X_left = X[row_indices] # equals the left-hand-side of (6)
3 X_right = X[col_indices] # equals the right-hand-side of (6)

```

Linear Algebra Notations. This study heavily relies on the Singular Value Decomposition (SVD) of matrices [Eckart and Young, 1936, Hestenes, 1958] e.g. $\mathbf{X} = \mathbf{U}_x \mathbf{\Sigma}_x \mathbf{V}_x^T$ that are denoted as the left singular vectors $\mathbf{U}_x \in \mathbb{R}^{N \times N}$, the singular values $\mathbf{\Sigma}_x \in \mathbb{R}^{N \times D}$ and the right singular vectors $\mathbf{V}_x \in \mathbb{R}^{D \times D}$ of $\mathbf{X} \in \mathbb{R}^{N \times D}$. We will always specify as a lower-script and lower-case the matrix that is being decomposed (x in this case). It will also be convenient to only consider the left/right singular vectors whose associated singular values are 0 that we will denote as $\bar{\mathbf{U}}_x$ and $\bar{\mathbf{V}}_x$ respectively. Conversely, the left/right singular vectors whose associated singular values are > 0 will be denote as $\hat{\mathbf{U}}_x$ and $\hat{\mathbf{V}}_x$ respectively. Lastly, we will denote by $\boldsymbol{\sigma}_z$ the vector of singular values such as $\mathbf{\Sigma}_z = \text{diag}(\boldsymbol{\sigma})$ and without loss of generality and unless otherwise stated, this will always be in descending order.

Our goal in the following sections (Section 3 for VICReg, Section 4 for SimCLR/NNCLR, and Section 5 for BarlowTwins) will be to find the optimal representations \mathbf{Z} of \mathbf{X} whilst tying those methods to their spectral

embedding counterpart. Three surprising facts will emerge: (i) all existing methods recover exactly some flavors of famous spectral method, (ii) the spectral properties of the optimal representation \mathbf{Z} of \mathbf{X} can be obtained in closed-form, and (iii) from those properties, necessary and sufficient conditions can be obtained to bound the downstream task error of those optimal SSL representations (Section 6).

3 VICReg Minimizes the Dirichlet Energy to Produce Smooth Signals on the Graph \mathbf{G} While Preventing Dimensional Collapse

We will first demonstrate in Section 3.1 that the optimal VICReg representation can be obtained in closed form (Theorem 1) and that turning the VICReg optimization as a constrained problem recovers (Kernel) Laplacian Eigenmaps, an eponymous spectral embedding method Section 3.2. We then consider that same constrained problem but under a linear network regime for which we obtain the closed-form optimal network’s parameters (Theorem 3) and in which case, VICReg recovers Locality Preserving Projections and Linear Discriminant Analysis (Section 3.3).

3.1 Closed-Form Optimal Representation for VICReg

The first goal of this section is to build up some insights into VICReg by demonstrating how the invariance term corresponds to the Dirichlet energy of the signal \mathbf{Z} on the graph \mathbf{G} . Then, replacing the variance hinge loss at 1 with the squared loss at 1 as in $\sum_{k=1}^K (1 - \text{Cov}(\mathbf{Z})_{k,k})^2$ —notice that minimizing the latter implies minimizing the former—we obtain the closed-form optimal representation \mathbf{Z}^* of \mathbf{X} which turns out to be a function only of \mathbf{G} and the loss’ hyper-parameters.

From invariance to trace minimization. As a first step, we propose to better understand the impact of VICReg’s invariance term (recall Eq. (2)) onto the left-singular vectors of the representation \mathbf{Z} . Recalling from Section 2 that we denote the SVD of \mathbf{Z} by $\mathbf{U}_Z \Sigma_Z \mathbf{V}_Z^T$ we obtain the following

$$\underbrace{(\mathbf{G})_{i,j} \|(\mathbf{Z})_{i,\cdot} - (\mathbf{Z})_{j,\cdot}\|_2^2}_{(i,j) \text{ invariance term in VICReg}} = (\mathbf{G})_{i,j} \|\Sigma_Z^T ((\mathbf{U}_Z)_{i,\cdot} - (\mathbf{U}_Z)_{j,\cdot})\|_2^2 \propto (\mathbf{G})_{i,j} \|\widehat{\mathbf{U}}_Z)_{i,\cdot} - (\widehat{\mathbf{U}}_Z)_{j,\cdot}\|_2^2, \quad \text{acts upon the rows of the left singular vector of } \mathbf{Z}$$

where we recall that $\widehat{\mathbf{U}}_Z$ are the left-singular vectors of \mathbf{Z} associated to nonzero singular values, and $(\mathbf{M})_{i,\cdot}$ extracts the i^{th} row viewed as a column vector, for any matrix \mathbf{M} . Hence, VICReg effectively minimizes the pairwise distance between the i^{th} and j^{th} rows of $\widehat{\mathbf{U}}_Z$ whenever $(\mathbf{G})_{i,j} > 0$. This connection can be made more precise by rewriting the invariance loss of VICReg as the energy of the signal \mathbf{Z} on the graph \mathbf{G} [Von Luxburg, 2007] since we have (derivations in Appendix A.5)

$$\underbrace{\sum_i \sum_j (\mathbf{G})_{i,j} \|(\mathbf{Z})_{i,\cdot} - (\mathbf{Z})_{j,\cdot}\|_2^2}_{\text{invariance term in VICReg}} = 2 \underbrace{\text{Tr}(\mathbf{Z}^T \mathbf{L} \mathbf{Z})}_{\text{Dirichlet energy of } \mathbf{Z} \text{ on } \mathbf{G}}, \quad (7)$$

where \mathbf{L} is the graph Laplacian matrix $\mathbf{L} = \mathbf{D} - \mathbf{G}$ with \mathbf{D} the diagonal degree matrix of \mathbf{G} i.e. $(\mathbf{D})_{i,j} = \sum_j (\mathbf{G})_{i,j}$ and $(\mathbf{D})_{i,j} = 0, \forall i \neq j$. From Eq. (7) it is clear that the invariance term depends on the matching between the left singular vectors of \mathbf{Z} and the eigenvectors of \mathbf{L} . Hence, *non-contrastive learning aims at producing non-degenerate signals \mathbf{Z} that are smooth on \mathbf{G} .*

Analytical optimal representation. To gain further insights into VICReg, we ought to obtain the analytical form of the optimal representation \mathbf{Z}^* minimizing Eq. (2)—although this optimum is not unique e.g. adding a constant entry to each column of \mathbf{Z} does not change the loss value (details in Appendix A.6). To that end, we will need to work with a slightly friendlier variance term i.e. we replace the hinge loss at 1 with the squared loss centered at 1 as in $\sum_{k=1}^K (1 - \text{Cov}(\mathbf{Z})_{k,k})^2$. We can now obtain the following characterization of \mathbf{Z}^* as a function of the spectral decomposition of the matrix that combines two Laplacian matrices (details in Appendix A.7). The first, (left of Eq. (8)) comes from the variance+covariance term is the Laplacian of a complete graph i.e. where each node/sample is connected all others, and the second (right of Eq. (8)) is the one of the graph described by \mathbf{G} as in

$$\underbrace{\mathbf{I} - \frac{1}{N} \mathbf{1}\mathbf{1}^T}_{\text{Laplacian of a complete graph}} - \frac{\gamma}{\alpha} \overbrace{(\mathbf{D} - \mathbf{G})}^{\text{Laplacian of the SSL/sup. graph}} = \mathbf{P}_{\alpha,\gamma} \text{diag}(\lambda_{\alpha,\gamma}) \mathbf{P}_{\alpha,\gamma}^T, \quad (8)$$

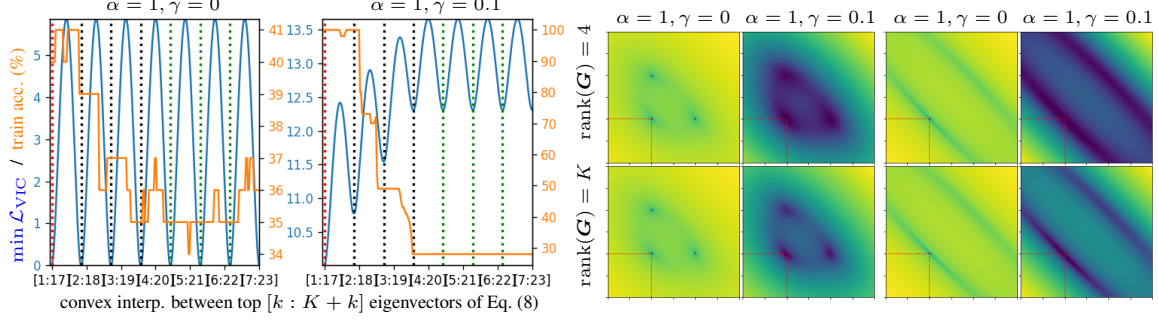


Figure 4: **Left:** depiction of the optimal VICReg loss with varying hyper-parameters (**blue line**) when the representation is formed from the top $[k : K + k]$ eigenvectors of Eq. (8) with convex interpolation in-between. Recall from Theorem 1 that the global optimum is given by the $[1 : K - 1]$ case. We also depict the downstream task performance (**orange line**) and we clearly observe that both are closely related as expected (see Theorem 9). Notice that since we are considering classification, even without the correct first eigenvector the linear classifier on top of $\mathbf{Z}_{\alpha,\gamma}^*$ is able to solve the task at hand thanks to the probability constraint that must sum to 1 i.e. the last component can be recovered from the first $C - 1$. **Right:** depiction of the loss landscape of \mathcal{L}_{VIC} around the optimal $\mathbf{Z}_{\alpha,\gamma}^*$ on the left using the directions provided by the top $[2 : K + 1]$ and $[3 : K + 2]$ eigenvectors of Eq. (8), and then with random directions in \mathbf{Z} -space. All experiments employed $N = 256$, $K = 16$, $\text{rank}(\mathbf{G}) = 4$.

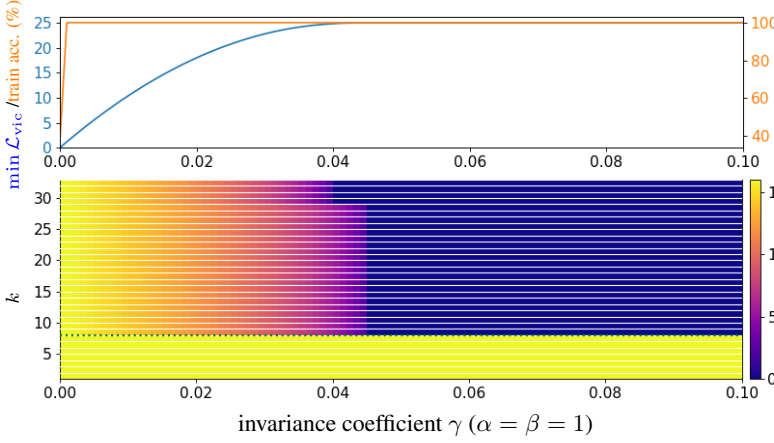


Figure 5: **Top:** the minimal VICReg loss (**blue line**) and corresponding downstream task performance (**orange line**). **Bottom:** evolution of $\mathbf{Z}_{\alpha,\gamma}^*$'s singular values. We observe that VICReg benefits from a (α, γ) -zone for which $\mathbf{Z}_{\alpha,\gamma}^*$ remains full rank and still incorporates enough information on \mathbf{G} to solve the downstream task. Hence, depending on the confidence one has into \mathbf{G} , one can adjust γ/α to either incorporate no information on \mathbf{G} , incorporate \mathbf{G} and maintain full-rank or entirely collapse to \mathbf{G} . All experiments employed $N = 256$, $K = 32$, $\text{rank}(\mathbf{G}) = 8$.

where the eigenvalues/eigenvectors are in descending orders. Combining the eigenvectors of the combined Laplacians will be used to produce the optimal VICReg representation as formalized below.

Theorem 1. A global minimizer of the VICReg loss ($\alpha = \beta, \forall \gamma$) denoted by $\mathbf{Z}_{\alpha,\gamma}^*$ is obtained from Eq. (8) along with the minimal achievable loss which are given by

$$\mathbf{Z}_{\alpha,\gamma}^* = (\mathbf{P}_{\alpha,\gamma}(\text{diag}(\boldsymbol{\lambda}_{\alpha,\gamma})N)^{1/2})_{:,1:K} \quad \text{and} \quad \min_{\mathbf{Z} \in \mathbb{R}^{N \times K}} \mathcal{L}_{\text{VIC}} = \alpha(K - \|(\boldsymbol{\lambda}_{\alpha,\beta})_{1:K}\|_2^2),$$

and any K -out-of- N columns of $\mathbf{P}_{\alpha,\gamma}(\boldsymbol{\Lambda}_{\alpha,\gamma}N)^{1/2}$ is a local minimum of \mathcal{L}_{VIC} . (Proof in Appendix A.7.)

The above result provides a few key insights. First, only the ratio γ/α governs the VICReg representation. Second, there exists many local minimum, some of which can be explicitly found by taking various K -out-of- N columns of $\mathbf{P}_{\alpha,\gamma}(\boldsymbol{\Lambda}_{\alpha,\gamma}N)^{1/2}$ which we display in Fig. 4 along with the loss landscape of \mathcal{L}_{VIC} around the optimal representation \mathbf{Z}^* . We also depict in Fig. 5 the evolution of the eigenvalues $(\boldsymbol{\lambda}_{\alpha,\gamma})_{1:K}$ for varying γ along with the downstream task (induced by \mathbf{G}) training performance. We observe that VICReg benefits from a sweet-spot where it can both preserve a full-rank representation \mathbf{Z}^* and incorporate enough information about \mathbf{G} to solve the task at hand perfect. As will become clear in Sections 4 and 5 this does not hold for all methods as SimCLR and BarlowTwins collapse the rank of \mathbf{Z}^* . We also depict on the left of Fig. 6 the convergence of the optimal representation of VICReg to the true one with different flavors of gradient descent. Beyond interpretability, Theorem 1 also clearly demonstrate the impact of \mathbf{G} on the quality of the obtained representation $\mathbf{Z}_{\alpha,\gamma}^*$. We will make the ability of $\mathbf{Z}_{\alpha,\gamma}^*$ to solve a downstream task at hand as a function of the spectrum of \mathbf{G} in Section 6.3.

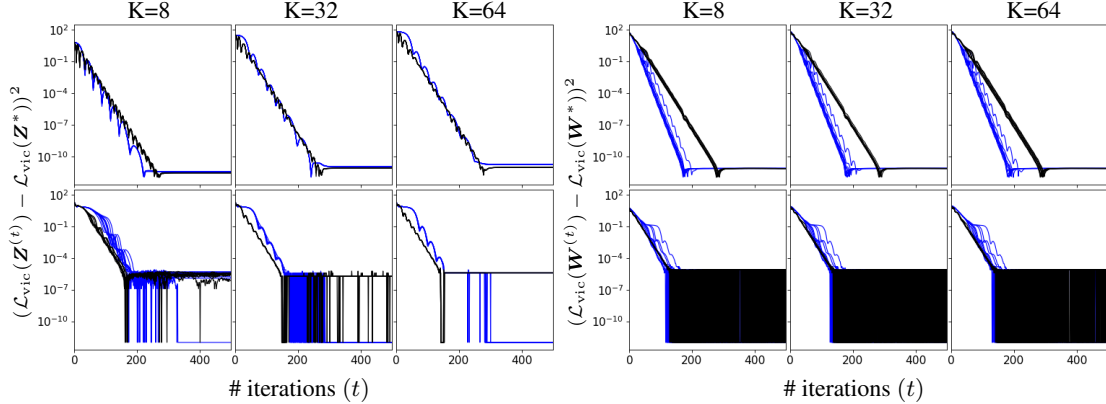


Figure 6: **Left:** depiction of the convergence between a randomly initialized representation \mathbf{Z} and the optimal one \mathbf{Z}^* from Theorem 1 measured as quadratic difference of the VICReg loss \mathcal{L}_{vic} . **Right:** depiction of the convergence between a random initialized linear weight matrix \mathbf{W} and the optimal one \mathbf{W}^* from Eq. (12) also measured as quadratic difference of the VICReg loss \mathcal{L}_{vic} . We employ $\alpha = 1, \gamma = 0$ on the **top row** and $\alpha = 1, \gamma = 0.01$ on the **bottom row** and $N=512, C=8, D=64$. In both cases, the **blue line** corresponds to RMSProp optimizer and the **black line** to SGD. Each setting is repeated 10 times and each line corresponds to a different random initialization. We observe that in both settings gradient based learning is able to produce a final representation (left) and linear weight (right) that match with the optimum ones found analytically for VICReg.

Computationally friendly solution. Before concluding this section we ought to recall that Eq. (8), which needs to be decomposed to obtain $\mathbf{Z}_{\alpha, \gamma}^*$ is a dense $N \times N$ matrix e.g. as follows

```

1 L = ch.diag(G.sum(1)) - G # Laplacian matrix L in Eq. 8
2 Lam, P = ch.linalg.eigh(torch.eye(N) - 1 / N - (gamma / alpha) * L) # equals to (8)
3 Z_star = P[:, -K:] * ((Lam[-K:] * N).sqrt()) # equals to Z* of Thm. 1
4 min_L = alpha * (K - Lam[-K:].norm().square()) # equals to min L_vic of Thm. 1

```

However, we can equivalently find the optimal VICReg solution $\mathbf{Z}_{\alpha, \gamma}^*$ only as a function of \mathbf{L} which is sparse e.g. for SSL \mathbf{L} contains $2N$ nonzero entries, and for supervised settings with C balanced classes, \mathbf{L} contains N^2/C nonzero entries. To do so, notice in Eq. (8) that the left term $\mathbf{I} - \frac{1}{N}\mathbf{1}\mathbf{1}^T$ mostly acts to ensure that the found eigenvectors with nonzero eigenvalues have 0 mean. Instead, we can achieve the same goal by defining the following *sparse and symmetric* matrix

$$\begin{pmatrix} 0 & \mathbf{1}^T \\ \mathbf{1} & \mathbf{I} - \frac{\gamma}{\alpha} \mathbf{L} \end{pmatrix} \in \mathbb{R}^{(N+1) \times (N+1)}, \quad (9)$$

and by taking the top $[2 : K]$ (and not $[1 : K - 1]$ as with Eq. (8)) eigenvectors. In short, while Eq. (8) was adding a connection from each node of the graph to all others, Eq. (9) introduces a new node to the graphs and connects it to all others, akin to the Hubbard-Stratonovich transformation [Hirsch, 1983]. The great advantage of Eq. (9) is the sparsity of the matrix allowing it to be easily stored and for which there exists efficient routines to rapidly obtain the top eigenvectors, even for large N . One popular solution is the Locally Optimal Block Preconditioned Conjugate Gradient [Knyazev, 1987] which only needs to evaluate matrix-vector products.

Prior to moving to other SSL methods, we first emphasize the ability of VICReg to recover *local* spectral methods in the following sections.

3.2 VICReg Recovers Laplacian Eigenmaps in Feature Space and Kernel Locality Preserving Projection in Data Space

From the previous section Theorem 1 and Eq. (8) we obtained that the ratio $\frac{\gamma}{\alpha}$ entirely controls the mixing between the Laplacian matrix of a complete graph and the one from \mathbf{G} . In other words, this ratio controls the spectral properties of $\mathbf{Z}_{\alpha, \gamma}^*$ by interpolating between the ones of $\mathbf{I} - \frac{1}{N}\mathbf{1}\mathbf{1}^T$ and the ones of \mathbf{L} (recall Fig. 5). The goal of this section is to study more precisely the scenario where $\alpha \gg \gamma$ i.e. we prioritize the variance-covariance terms, in which case VICReg recovers Laplacian Eigenmaps (LE) [Belkin and Niyogi, 2003] in feature space, and kernel Locality Preserving Projection (kLPP) [He and Niyogi, 2003] in data space.

In feature space. LE is a non-parametric method searching for a representation \mathbf{Z} by minimizing the following Brockett [Brockett, 1991] optimization problem

$$\min_{\mathbf{Z}} \text{Tr}(\mathbf{Z}^T (\mathbf{D} - \mathbf{G}) \mathbf{Z}) \text{ s.t. } \mathbf{Z}^T \mathbf{D} \mathbf{Z} = \mathbf{I}, \quad (10)$$

with \mathbf{D} the diagonal degree matrix of \mathbf{G} (recall Eq. (8)). The relation between Eq. (10) and VICReg comes by combining the following two facts. First, minimizing Eq. (10) is done by taking the eigenvectors associated to the K smallest eigenvalues of $\mathbf{I} - \mathbf{D}^{-1} \mathbf{G}$ (see Liang et al. [2021] and Corollary 4.3.39 from Horn and Johnson [2012]) yet, —LE disregards the eigenvector associated to the eigenvalue 0— to produce the optimal LE solution denoted as \mathbf{Z}_{LE}^* . Doing so, Belkin and Niyogi [2003] produced a representation whose columns have 0-mean since the only eigenvector with nonzero mean is the one associated to the eigenvalue 0 (details in Appendix A.8). Second, VICReg employs a graph \mathbf{G} for which $\mathbf{D} = c\mathbf{I}$ with $c = 2$ (positive pairs), $c = 3$ (positive triplets, and so on. And thus, the eigenvectors associated to the nonzero eigenvalues of $\mathbf{D} - \mathbf{G}$ or $\mathbf{I} - \mathbf{D}^{-1} \mathbf{G}$ are the same i.e. the optimal solution of the LE problem minimizes the VICReg criterion with strict enforcement that the variance+covariance terms, denoted as $\mathcal{L}_{\text{var}}, \mathcal{L}_{\text{cov}}$ hereon, are zero.

Theorem 2. *Given a dataset \mathbf{X} and relation matrix \mathbf{G} , minimizing the VICReg loss (Eq. (2)) with constraint that the variance and covariance loss are 0 (α, β become irrelevant) as in*

$$\mathcal{L}_{\text{vic}}(\mathbf{Z}_{\text{LE}}^*) = \min_{\mathbf{Z} \in \mathbb{R}^{N \times K}} \mathcal{L}_{\text{inv}}(\mathbf{Z}) \text{ s.t. } \mathcal{L}_{\text{var}} = 0 \text{ and } \mathcal{L}_{\text{cov}} = 0.$$

(Proof in Appendix A.8.)

Hence, given a relation matrix \mathbf{G} , solving the LE problem is equivalent to solving a constrained VICReg problem. We ought to highlight however that a crucial part of LE lies in the design of that matrix \mathbf{G} , often found from a k -NN graph [Hautamaki et al., 2004] of the samples \mathbf{X} in the input space, while in SSL it is constructed from data-augmentations or given.

Going beyond LE, one can easily obtain that if $(\mathbf{D} - \mathbf{G})$ is idempotent —which is true for common supervised and SSL scenarios as \mathbf{G} corresponds to a union of complete graphs— then LE also corresponds to Locally Linear Embedding [Roweis and Saul, 2000] and so does VICReg.

In data space. One difficulty arising from LE, and from non-parametric methods in general, is the ability to produce new representations \mathbf{z} for new data samples that were not present when solving Eq. (10). This led to the development of a two-step modeling process as

$$\mathbf{x} (\in \mathbb{R}^D) \mapsto \mathbf{h} = \phi(\mathbf{x}) (\in \mathbb{R}^S) \mapsto \mathbf{z} = \mathbf{W}^T \mathbf{h} (\in \mathbb{R}^K),$$

with $S \gg K$, $\mathbf{W} \in \mathbb{R}^{S \times K}$, and where the first mapping’s goal is to learn a generic input embedding that can be reused on new samples \mathbf{x} . To see this, let’s collect those mappings for all the training set into the $N \times S$ matrix Φ . With that, the LE problem in data space —known as the Kernel Locality Preserving Projection problem— becomes

$$\min_{\theta: \mathbf{W}^T \Phi^T \mathbf{D} \Phi \mathbf{W} = \mathbf{I}} \text{Tr}(\mathbf{W}^T \Phi^T (\mathbf{D} - \mathbf{G}) \Phi \mathbf{W}), \quad (11)$$

so that the original LE representation \mathbf{Z} can be obtained simply as $\mathbf{Z} = \Phi \mathbf{W}$. And more importantly, given a new sample \mathbf{x} , one can simply obtain the new representation via $\mathbf{z} = \mathbf{W}^T \phi(\mathbf{x})$.

Most existing solutions have been leveraging the Moore-Aronszajn theorem [Aronszajn, 1950] and the fact that we are in a finite data regime to shift the question *what nonlinear and high-dimensional operator ϕ should be used?* to the perhaps simpler question *what symmetric positive (semi-)definite matrix $\Phi \Phi^T$, i.e. what kernel, function should be used?* [Bengio et al., 2003, Cheng et al., 2005, Tai et al., 2022]. Doing so, $\mathbf{W}^T \phi(\mathbf{x})$ can now be easily implemented e.g. as a Generalized Regression Network [Broomhead and Lowe, 1988, Specht et al., 1991]. The crucial result of interest for our study is the following one that combine Theorem 2 with a result from He and Niyogi [2003] demonstrating the equivalence between LE in feature space and KLLLE in data space.

Proposition 1. *VICReg with variance/covariance constraint solves LE in embedding space and KLLLE in input space (recall Eq. (11)) employing a DN for $\mathbf{W}^T \circ \phi$.*

Equipped with those results, we can now propose a practical result by obtaining in closed-form the optimal parameter weights that solve the constrained VICReg criterion with a linear network.

3.3 With a Linear Network VICReg Recovers Locality Preserving Projections and Linear Discriminant Analysis with Analytical Optimal Network Parameters

The goal of this section is to focus on the linear case i.e. $Z = XW$. In that setting, and still employing the squared variance term as in Theorem 3, VICReg recovers two known spectral methods: Locality Preserving Projections (LPP) [He and Niyogi, 2003] for an arbitrary relation matrix G , and Linear Discriminant Analysis (LDA) [Fisher, 1936, Cohen et al., 2014] when G is the supervised relation matrix. In both cases we obtain the analytical form of the optimal weights W .

Prior connecting linear VICReg to LPP and LDA we ought to highlight the optimal weights W^* of the linear VICReg model (derivations in Appendix A.9) given by

$$W^* = \left(\text{Cov}(X)^{-1} \left(\text{Cov}(X) - \frac{\gamma}{\alpha N} X^T L X \right)^{\frac{1}{2}} \right)_{:,1:K}, \quad (12)$$

which is easily computed as

```
1 cov = torch.cov(X.t(), correction=0) # cov. w/o correction (otherwise scale L by (N-1))
2 B = cov - (gamma / (N * alpha)) * (X.t() @ L @ X)
3 Wstar = torch.linalg.solve(A, sqrtm(B)) # numerically stable solution of 12, sqrtm(B)=sqrt(B)
```

and we depict the gradient convergence towards this optimal solution is depicted on the right of Fig. 6.

We now turn to connecting linear VICReg to LPP and LDA, heavily relying on Theorem 2. In fact, we already saw that VICReg with a DN corresponds to the Kernel LE methods. In the linear regime, it is already established that kernel LE recovers LPP. The perhaps less direct result concerns the recovery of LDA for which we first need to introduce the supervised counterpart of G . In that case, G describes the known class relation from $y \in \{1, \dots, C\}^N$ as in

$$(G_s)_{i,j} = 1_{\{(y)_i=(y)_j\}} 1_{\{i \neq j\}}, \quad (\text{supervised } G) \quad (13)$$

which can be directly computed as

```
1 Gs = torch.eq(target, target[:, None]).float() - torch.eye(N) # equals to Eq. 13
```

Note that the degree matrix of G_s will contain for each diagonal entry i the number of samples that belong to the class $(y)_i$ of sample i .

Theorem 3. *Variance-covariance constrained VICReg (recall Theorem 2) with a linear network ($K \leq D$) recovers LPP, and LDA (with G_s from Eq. (13) and $K = C$). In both cases the optimal parameter W^* is given by the top- K eigenvectors of $(X^T(D - G)X)^{-1}X^T G X$ with $G \mapsto G_s$ for LDA. (Proofs in Appendices A.14 and A.15.)*

Interestingly, the eigenvalues associated to the eigenvectors of W^* exactly recover the multivariate analysis of variance (MANOVA) sufficient statistics of the data [O'Brien and Kaiser, 1985, Huberty and Olejnik, 2006]. Hence, although not further explored in this study, we believe that important statistical results could be further obtained e.g. to assess the goodness-of-fit of the model without requiring a downstream task [Mika et al., 1999, Ioffe, 2006, Xue and Hall, 2014].

After a thorough analysis of VICReg we now propose to turn to another important SSL loss which is SimCLR, and its variants.

4 SimCLR/NNCLR/MeanShift Solve a Generalized Multidimensional Scaling Problem à la ISOMAP

Recall from Section 2 and Eq. (3) that the SimCLR loss first computes a similarity matrix \hat{G} of some flavor that depends on the representation Z , and then compares it against the known data relation G . Different G matrices lead to different variants of SimCLR [Chen et al., 2020] such as NNCLR [Dwivedi et al., 2021] or MeanShift [Koohpayegani et al., 2021], hence making our results general. The goal of this section is two-fold. First, we demonstrate that different $Z \mapsto \hat{G}$ mappings solve different optimization problems (Theorem 4) —all trying to estimate the similarity matrix G from the signals Z akin to Laplacian estimation in Graph Signal Processing. Second, we demonstrate that SimCLR and its variants force Z 's spectrum to align with the one of G (through \hat{G}) akin to the ISOMAP method, by means of a Multi-Dimensional Scaling solution (Proposition 2).

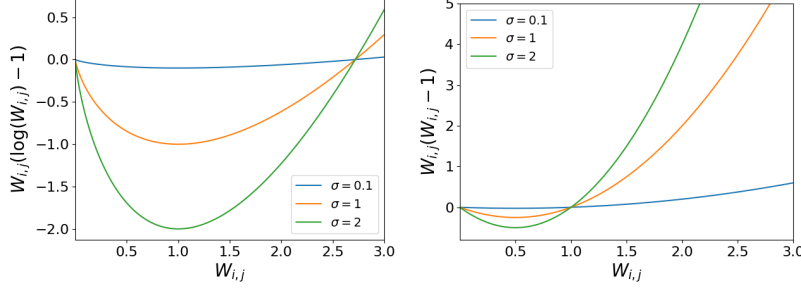


Figure 7: Depiction of the regularization term \mathcal{R}_{\log} (left) and \mathcal{R}_{log} (right) from Eq. (15) for varying value of $(\mathbf{W})_{i,j}$ and three different temperatures $\tau \in \{0.1, 1, 2\}$ demonstrating how such regularization prevents $\hat{\mathbf{G}}$ to collapse to the trivial 0 matrix in the optimization problem in Eq. (14).

4.1 Step 1: SimCLR Pairwise Similarities Solve a Graph Laplacian Estimation Problem

Let’s first define the minimization problem that given a set of signals i.e. rows of \mathbf{Z} produces a relation estimate $\hat{\mathbf{G}}$ of \mathbf{G} . To ease notations, we gather in the $N \times N$ matrix \mathbf{D} all the pairwise distances $(\mathbf{D})_{i,j} = d(f_{\theta}(\mathbf{x}_i), f_{\theta}(\mathbf{x}_j))$ with d any preferred metric. The standard problem of estimating $\hat{\mathbf{G}}$ from \mathbf{Z} can be cast as an optimization problem [Dong et al., 2016, Kalofolias, 2016] as

$$\hat{\mathbf{G}}_{d,\mathcal{R}} = \arg \min_{\mathbf{G} \in \mathcal{G}} \sum_{i,j} d(f_{\theta}(\mathbf{x}_i), f_{\theta}(\mathbf{x}_j))(\mathbf{G})_{i,j} + \mathcal{R}(\mathbf{G}) = \arg \min_{\mathbf{G} \in \mathcal{G}} \text{Tr}(\mathbf{D}\mathbf{G}) + \mathcal{R}(\mathbf{G}), \quad (14)$$

with \mathcal{G} the set (or subset) of symmetric matrices with nonnegative entries and zero diagonal, and with \mathcal{R} a regularizer preventing $\hat{\mathbf{G}}$ to be the trivial zero matrix e.g.

$$\mathcal{R}_{\log}(\mathbf{G}) = \sum_{i \neq j} \tau \mathbf{G}_{i,j} (\log(\mathbf{G}_{i,j}) - 1) \quad \text{or} \quad \mathcal{R}_{\text{F}}(\mathbf{G}) = \sum_{i \neq j} \tau \mathbf{G}_{i,j} (\mathbf{G}_{i,j} - 1). \quad (15)$$

We provide in Fig. 7 a depiction of the impact of $\mathcal{R}(\mathbf{G})$ which pushes the entries of the weight matrix to be close to 1 with strength depending on the temperature parameter τ .

Hence $\hat{\mathbf{G}}$ from Eq. (14) is the optimal graph—expressed as a weight matrix—for which the signal $\mathbf{Z} = f_{\theta}(\mathbf{X})$ on that graph is smooth. For example one can solve Eq. (14) only on $\mathcal{G}_{\text{rsto}}$, the space of right-stochastic matrices i.e. a subset of \mathcal{G} that only contains matrices whose rows sum to 1 i.e. $\mathcal{G}_{\text{rsto}} = \{\mathbf{G} \in \mathcal{G} : \mathbf{G}\mathbf{1} = \mathbf{1}\}$. We now propose the first formal result that ties the estimate $\hat{\mathbf{G}}$ from Eq. (14) to the one of SimCLR/NNCLR/MeanShift whenever the regularizer \mathcal{R} is given by but with different spaces for \mathbf{G} .

Theorem 4. Using \mathcal{R} from Eq. (15) leads to the following graph weight estimate

$$\begin{aligned} (\hat{\mathbf{G}}_{d,\mathcal{R}_{\log}})_{i,j} &= e^{-\frac{1}{\tau} d(f_{\theta}(\mathbf{x}_i), f_{\theta}(\mathbf{x}_j))} \mathbf{1}_{\{1 \neq j\}}, & (\text{with } \mathcal{G}) \\ (\hat{\mathbf{G}}_{d,\mathcal{R}_{\log}})_{i,j} &= \frac{e^{-\frac{1}{\tau} d(f_{\theta}(\mathbf{x}_i), f_{\theta}(\mathbf{x}_j))}}{\sum_{j \neq i} e^{-\frac{1}{\tau} d(f_{\theta}(\mathbf{x}_i), f_{\theta}(\mathbf{x}_j))}} \mathbf{1}_{\{1 \neq j\}}, & (\text{with } \mathcal{G}_{\text{rsto}}) \end{aligned} \quad (16)$$

and thus if d is the cosine distance, Eq. (16) recovers SimCLR similarity estimate, and if d is the ℓ_2 distance, Eq. (16) recovers the Lifted Structured Loss [Weinberger and Saul, 2009]. (Proof in Appendix A.10.)

The above result plays a crucial role as it motivates the need to better understand SSL from a theoretical perspective. Based on this maximization principle, we can now obtain novel variations of SimCLR by solving Eq. (14) with different constraints. For example one could obtain (derivations in Appendix A.10) the following variations that are akin to the quantities used in Hadsell et al. [2006], Weinberger and Saul [2009] i.e. with the ℓ_2 distance and no exponentiation

$$\hat{\mathbf{G}}_{d,\mathcal{R}_{\text{F}}} = \text{ReLU}(\mathbf{1}\mathbf{1}^T - \mathbf{I} - \mathbf{D}/\tau), \quad (\text{with } \mathcal{G}, \tau > 0), \quad (17)$$

$$\hat{\mathbf{G}}_{d,\mathcal{R}_{\text{F}}} = \text{ReLU}\left(\frac{1}{N-1}(\mathbf{1}\mathbf{1}^T - \mathbf{I}) - \frac{1}{\tau}\mathbf{D}\left(\mathbf{I} - \frac{1}{N-1}\mathbf{1}\mathbf{1}^T\right)\right), \quad (\text{with } \mathcal{G}_{\text{rsto}}, \tau > 0). \quad (18)$$

Now that we have demonstrated how SimCLR estimates the graph at hand, the next section will focus on the second step: matching $\hat{\mathbf{G}}$ to \mathbf{G} .

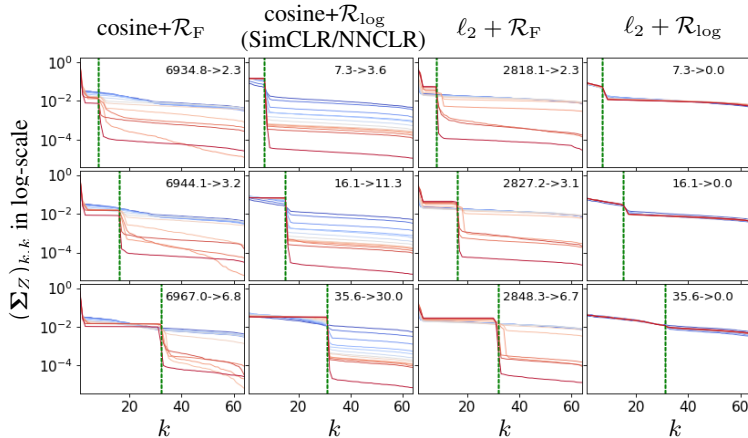


Figure 8: Depiction of the singular values Σ_Z of the representation Z learned by the SimCLR/NNCLR loss with $\mathcal{G}_{\text{rsto}}$, varying $\text{rank}(\mathbf{G}) \in \{8, 16, 32\}$ (rows, green dotted lines) and evolution during training (from blue to red, number in top-right corner) with various (d, \mathcal{R}) configurations (columns, recall Theorem 4). We observe that the rank of the learned representation matches exactly the one of \mathbf{G} validating the result from Theorem 5 regardless of the chosen hyper-parameters, making SimCLR’s performances more sensitive to the design of \mathbf{G} than methods like VICReg whose representation preserves remains full-rank (recall Fig. 5).

4.2 Step 2: SimCLR Fits the Estimated Graph $\hat{\mathbf{G}}$ to the Known Graph \mathbf{G}

SimCLR’s first step produced a graph estimate $\hat{\mathbf{G}}$ from Z . The second step now consists in measuring how fit is this estimate compared to \mathbf{G} , so that the model’s parameters can be tuned to increase this fitness. We demonstrate in this section that in doing so, SimCLR forces Z to have the same nonzero left singular vectors as the nonzero eigenvectors of \mathbf{G} , and that as opposed to VICReg, the rank between Z and \mathbf{G} matches.

The method used to compare $\hat{\mathbf{G}}$ and \mathbf{G} should reflect the properties fulfilled by those matrices e.g. being doubly-stochastic or right-stochastic and the type of measure one aims to impose. In all generality, let’s denote the SimCLR comparison method to be one of the two following variants (depending on the type of constraints put on $\hat{\mathbf{G}}$ and \mathbf{G}

$$\mathcal{L}_{\text{SimCLR}} = \begin{cases} \|\mathbf{G} - \hat{\mathbf{G}}(Z)\|_F^2, & \text{(Euclidean)} \\ -\text{Tr}\left(\left(\text{diag}(\mathbf{G}\mathbf{1})^{-1}\mathbf{G}\right)^T \log\left(\text{diag}(\hat{\mathbf{G}}(Z)\mathbf{1})^{-1}\hat{\mathbf{G}}(Z)\right)\right), & \text{(Cross-Entropy)} \end{cases}, \quad (19)$$

where the log is applied element-wise. When minimizing Eq. (19), SimCLR learns an embedding Z so that its graph estimate $\hat{\mathbf{G}}$ matches closely the known graph \mathbf{G} . To formalize below the form of the optimal SimCLR representation, we first ought to recall that we denote by \mathbf{U}_G and Σ_G the left singular vectors and singular values of \mathbf{G} respectively. Notice that since \mathbf{G} is symmetric semi-definite positive, \mathbf{U} also corresponds to its eigenvectors and Σ_G^2 to its eigenvalues.

Theorem 5. A global minimizer of the SimCLR loss denoted by Z^* along with the minimal achievable loss using Eq. (17) or Eq. (18), $\tau \geq \max_{i,j}(D)_{i,j}$ and with the LHS of Eq. (19) are given by

$$Z_\tau^* = (\mathbf{U}_G \Sigma_G^{1/2})_{:,1:K} \quad \text{and} \quad \min_{Z \in \mathbb{R}^{N \times K}} \mathcal{L}_{\text{SimCLR}} = \sum_{k=K+1}^N (\Sigma_G^2)_{k,k},$$

up to permutations of the singular vectors associated to the same singular value, and regardless of the loss and graph estimation, the rank of Z_τ^* is given by $\min(K, \text{rank}(\mathbf{G}))$. (Proof in Appendix A.11.)

We illustrate the above theorem for many combinations of distances and regularizers in Fig. 8 where we see that in all cases, SimCLR forces the representations Z to have a dimensional collapse, a phenomenon first observed in Hua et al. [2021] and that has been one of the unanswered phenomenon in SSL [Arora et al., 2019, Tosh et al., 2021]. In our goal to unify SSL methods under the realm of spectral embedding methods, we now propose the following section that ties SimCLR and its variants to *global* spectral methods.

4.3 SimCLR is Akin to ISOMAP in Feature Space and Kernel ISOMAP in Input Space

We now propose to tie the SimCLR method along with its variants e.g. NNCLR to known *global* spectral methods, e.g. ISOMAP [Tenenbaum et al., 2000] contrasting from VICReg which was tied to *local* spectral methods (recall Sections 3.2 and 3.3).

In feature space. Let’s first recall that ISOMAP is a variation of Multi-Dimensional Scaling (MDS) [Kruskal, 1964] also known as Principal Coordinates Analysis. Classical MDS tries to learn embedding vectors that

have similar pairwise distance (usually ℓ_2) than the pairwise distance of the given input data. Often, MDS does this by using similarities instead of distances and thus by solving the following optimization problem $\min_{\mathbf{Z}} \|\mathbf{G} - \mathbf{Z}\mathbf{Z}^T\|_F^2$, where \mathbf{G} is the Gram matrix of the inputs i.e. $\mathbf{G} = \mathbf{X}\mathbf{X}^T$. At the most general level, ISOMAP simply corresponds to solving that same optimization problem but after redefining \mathbf{G} to better capture the geometric information of \mathbf{X} e.g. using the shortest path distance of the k -NN graph of \mathbf{X} [Preparata and Shamos, 2012]. The surprising result that we formalize below is that SimCLR and in particular NNCLR recover ISOMAP, the former by prescribing \mathbf{G} given the known positive pairs, and the latter by building a nearest neighbor graph.

Proposition 2. *Using the settings of Theorem 5, SimCLR recovers a Generalized MDS akin to ISOMAP (and MDS iff $\mathbf{G} = \mathbf{X}\mathbf{X}^T$). (Proof in Appendix A.12.)*

In data space with DNs. From the above, we can extend Proposition 2 but in input space, in a very similar way as was done in Section 3.2. In fact, originating in Webb [1995], there was a search to extend MDS, and ISOMAP to an input space formulation to solve the out-of-bag problem. In this setting, and taking MDS as an example, the original similarity matrix $\mathbf{Z}\mathbf{Z}^T$ is replaced with $\Phi\mathbf{W}^T\mathbf{W}\Phi^T$ using the same notations as in Eq. (11) and already known relationship between those models, we obtain the following.

Proposition 3 ([Williams, 2000]). *Whenever SimCLR recovers ISOMAP or MDS in feature space, it recovers kernel ISOMAP or kernel PCA [Schölkopf et al., 1998] in input space.*

We will now turn to BarlowTwins, another non-contrastive method akin to VICReg (both of which fall back to LDA in the linear regime and with supervised \mathbf{G}).

5 BarlowTwins Solves a (Kernel) Canonical Correlation Analysis Problem and Can Recover VICReg

Our last step in our journey to unify SSL methods under spectral embedding methods deals with BarlowTwins. Akin to the development for VICReg and SimCLR, BarlowTwins will also fall back to a known spectral method in embedding space (Section 5.1) and in data space (Section 5.2) where in the later case we again obtain the close-form optimal network parameters in the linear regime.

5.1 BarlowTwins Recovers Kernel Canonical Correlation Analysis

Recall from Section 2 and Eq. (5) that the BarlowTwins loss is based on a cross-correlation matrix between positive pairs of samples. As we did for VICReg and SimCLR, our goal here is to tie BarlowTwins to a known spectral method known as Kernel Canonical Correlation Analysis.

There exists many different ways to formulate the CCA problem, we present one here in the linear regime to simplify notations based on Cunningham and Ghahramani [2015]. The goal of (linear) CCA is to learn pairs of filters that produce maximally correlated features as in

$$\max_{\mathbf{W}_a \in \mathbb{R}^{D_a \times K}, \mathbf{W}_b \in \mathbb{R}^{D_b \times K}} \frac{\text{Tr}(\mathbf{W}_a^T \Sigma_{ab} \mathbf{W}_b)}{\sqrt{\text{Tr}(\mathbf{W}_a^T \Sigma_{aa} \mathbf{W}_a) \text{Tr}(\mathbf{W}_b^T \Sigma_{bb} \mathbf{W}_b)}}, \text{ s.t. } \begin{cases} \frac{1}{N} \mathbf{W}_a^T \Sigma_{aa} \mathbf{W}_a = \mathbf{I} \\ \frac{1}{N} \mathbf{W}_b^T \Sigma_{bb} \mathbf{W}_b = \mathbf{I} \\ \mathbf{W}_a^T \Sigma_{ab} \mathbf{W}_b = \Lambda, \end{cases} \quad (20)$$

with Λ a diagonal ($K \times K$) matrix, and with $\Sigma_{aa} = \mathbf{X}_a^T \mathbf{X}_a$, $\Sigma_{ab} = \mathbf{X}_a^T \mathbf{X}_b$ and so on. We thus observe that Eq. (20) is the BarlowTwins objective of Eq. (5) up to rescaling of the weight matrices, as CCA aims to make $\mathbf{W}_a^T \Sigma_{ab} \mathbf{W}_b = \mathbf{W}_a^T \mathbf{X}_a^T \mathbf{X}_b \mathbf{W}_b = \mathbf{Z}_a^T \mathbf{Z}_b = \Lambda$ diagonal with maximal diagonal entries.

Going to the nonlinear regime i.e. kernel CCA follows directly by employing $\phi(\mathbf{x})$ embeddings of the input observations in-place of the inputs. We thus obtain the following result that nicely parallels with the ones we obtained for VICReg and SimCLR. In data space, BarlowTwins can be regarded (put in perspective with Section 5.2) as a nonlinear canonical correlation analysis (NLCA) [Dauxois and Nkiet, 1998] and in particular Kernel CCA (KCCA) [Lai and Fyfe, 2000, Fukumizu et al., 2007] akin to how VICReg recovered Kernel Locality Preserving Projection and SimCLR Kernel ISOMAP. We leverage the same notations as in Section 3.2.

Theorem 6. *BarlowTwins recovers Kernel Canonical Correlation Analysis with a DN as the featurizer ϕ and produce a representation with rank $\min(K, D, \text{rank}(\mathbf{G}))$. (Proof in Appendix A.13.)*

In addition to the above, we can obtain further interpretation of the components of BarlowTwins loss. For example, notice that Eq. (20) is only well-defined if $K < \min(D_a, D_b)$. This limitation led to ridge-type CCA

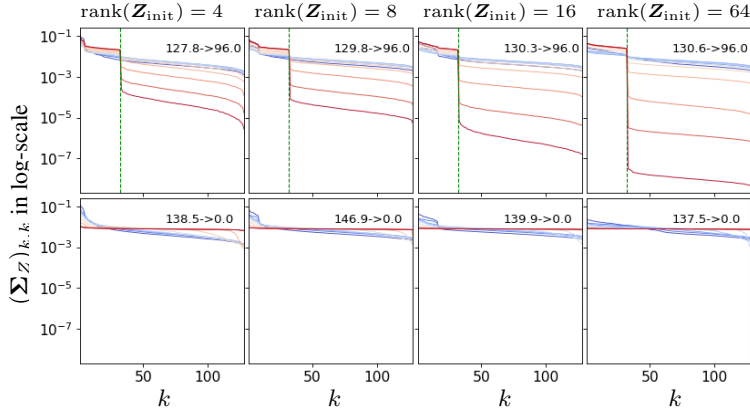


Figure 9: Depiction of the singular values Σ_Z of the representation Z learned by the BarlowTwins loss with Z_a, Z_b formed from Eq. (6) given G with $\text{rank}(G) \in \{32, 128\}$ (rows, green dotted lines) and with $N=512, K=128$ during training (from blue to red, number in top-right corner) with various initialization of Z (columns). We observe that the rank of the learned representation matches exactly the one of G validating the result from Theorem 6 regardless of the chosen hyper-parameters, making BarlowTwins’s performances more sensitive to the design of G akin to SimCLR and opposite to VICReg whose representation preserves full-rank (recall Fig. 5) when tuning the invariance parameter.

regularization which as been introduced in Gretton et al. [2005] as a mean to introduce numerical stability which in the context of linear CCA has been introduced by Vinod [1976] under the name *canonical ridge* and recovers exactly the addition of the ϵ constant in the denominator of the BarlowTwins loss in Eq. (5).

The above statement also brings yet another flavor of SSL methods. In fact, where VICReg allows to control the rank of Z to be in-between K and $\text{rank}(G)$ through the loss hyper-parameters, BarlowTwins and SimCLR enforce the rank of Z to be exactly the rank of G . We depict in Fig. 9 the evolution of $\text{rank}(Z)$ depending on the rank of the initialized representation $\text{rank}(Z_{\text{init}})$ using a gradient descent optimizer. We see that regardless of the initial rank of Z_{init} , training the representation to minimize the BarlowTwins loss makes the representation dimension collapse. Lastly, although not further studied here, we should point out to the reader that regularized forms of KCCA can be shown to include kernel ridge regression and regularized kernel Fisher LDA as special cases [Kuss and Graepel, 2003], further tying the special cases for which different SSL methods would fall back to the same model.

In the following section we will demonstrate how BarlowTwins in the linear regime exactly recovers Canonical Correlation Analysis.

5.2 With a Linear Network BarlowTwins Recovers Canonical Correlation Analysis and Linear Discriminant Analysis

The goal of this section is to further demonstrate the benefits of connecting SSL methods to spectral methods by exploiting the known techniques of the latter to help answer questions on the former.

As was done VICReg (we use linear settings of Section 3.2), we now obtain the optimal weights for BarlowTwins in the linear regime. We can even provide additional insights in this case since BarlowTwins is often seen as a key method that allows the use of different parameters/architectures to process X_a and X_b . We now show under what conditions on G sharing parameters is sufficient by first demonstrating how BarlowTwins recovers exactly CCA, and even LDA for supervised G . To streamline notations, we assume that our data is already centered, and thus define the covariance and cross-covariance matrices as $C_{aa} = X_a^T X_a, C_{lr} = X_a^T X_b$ and so on.

Theorem 7. *In the linear regime BarlowTwins recovers CCA with optimal weights given by*

$$W_a^* = \text{top-}K \text{ eigenvectors of } C_{aa}^{-1} C_{ab} C_{bb}^{-1} C_{ba} \text{ and } W_b^* = C_{bb}^{-1} C_{ba} W_a^*,$$

and (i)—with a symmetric G and same dimensional X_a, X_b , weight-sharing naturally occurs—as the optimal weights are $W_a^* = W_b^* = \text{top-}K \text{ eigenvectors of } C_{bb}^{-1} C_{ba}$ and (ii) if G is supervised and $K = C$ then BarlowTwins recovers LDA and thus VICReg (recall Theorem 3). (Proof in Appendix A.16.)

```

1 Caa = Xa.t() @ Xa + torch.eye(Da) * gamma # X_a ∈ ℝ^{N,D_a} regularized with gamma (γ)
2 Cbb = Xb.t() @ Xb + torch.eye(Db) * gamma # X_b ∈ ℝ^{N,D_b} regularized with gamma (γ)
3 RH = torch.block_diag(Caa, Cbb) # preparing the generalized eigenvalue prob.
4 LH = torch.block_diag(Xa.t() @ Xb, Xb.t() @ Xa).roll(Da, 1)
5 _, eigvecs = torch.lobpcg(LH, k=K, B=RH, niter=-1) # fast iterative solver

```

```

6 Wa, Wb = eigvecs.split([Da, Db])
7 Za = Xa @ Wa #  $Z_a \in \mathbb{R}^{N,K}$ 
8 Zb = Xb @ Wb #  $Z_b \in \mathbb{R}^{N,K}$ 

```

The above result opens new venues to extend current SSL methods (BarlowTwins in this case). For example, penalized matrix decomposition (PMD) from Witten et al. [2009] formulates a novel sparse formulation of CCA. In our context, this could lead to a new variation of BarlowTwins, in both the linear and nonlinear regimes. With the above results, we now connected most SSL methods to spectral methods, and found key properties that their representations/parameters inherit.

We now move away from connecting SSL methods to spectral methods, and finding the properties that their representations/parameters would inherit, to instead exploit those results and understand how well those learned representations can be to solve downstream tasks.

6 Optimality of Self-Supervised Methods to Solve Downstream Tasks

The goal of this section is to answer the following question: *given a task —encoded as a target matrix— $\mathbf{Y} \in \mathbb{R}^{N \times C}$, what are the sufficient statistics of \mathbf{Y} that a representation $\mathbf{Z} \in \mathbb{R}^{N \times K}$ must preserve to ensure that $\min_{\mathbf{W}, \mathbf{b}} \|\mathbf{Y} - \mathbf{Z}\mathbf{W} - \mathbf{b}\|_F^2 = 0$.* The first Section 6.1 will derive the optimal linear parameters (possibly non-unique) that minimize that loss, and will highlight the spectral properties of \mathbf{Y} that must be consistent in \mathbf{Z} . From that, Section 6.2 will be able to provide necessary and sufficient conditions for \mathbf{Z} to be optimal—in term of its left-singular vectors— and finally, Section 6.3 extends the recent studies of Bao et al. [2021a], HaoChen et al. [2021, 2022] to multiple SSL methods by demonstrating how and when SSL representations are optimal for downstream tasks.

6.1 Characterizing a Representation Usefulness by its Ability to Linearly Solve a Task

The goal of this section is to characterize the (possibly non-unique) parameter \mathbf{W} of the linear transformation that given any target matrix \mathbf{Y} and representation \mathbf{Z} minimize the Mean-Squared Error (MSE). Results in this section are standard in the linear algebra literature e.g. see Golub and Reinsch [1971] but we include it for completeness. We should also highlight that although for classification the cross-entropy loss is more common, it has recently been showed that ℓ_2 could perform as well [Hui and Belkin, 2020] with the correct parameter tuning, even on large models e.g. on the Imagenet dataset with modern deep learning architectures. Hence, we will leverage that loss function throughout this section.

Hence we consider that we are given representations $\mathbf{z} \triangleq f(\mathbf{x})$ from an input sample \mathbf{x} . Hence, we will denote the dataset representation as $\mathbf{Z} = [f(\mathbf{x}_1), \dots, f(\mathbf{x}_N)]^T \in \mathbb{R}^{N \times K}$ given a dataset $\mathbb{X} \triangleq \{\mathbf{x}_1, \dots, \mathbf{x}_N\}$, $N \in \mathbb{N}^*$. We are also given a task —encoded as a target matrix— $\mathbf{Y} \triangleq [\mathbf{y}_1, \dots, \mathbf{y}_N]^T \in \mathbb{R}^{N \times C}$ where each \mathbf{y}_n is associated to each input \mathbf{x}_n .

Without loss of generality and to lighten our derivations, we will omit the bias vector \mathbf{b} , it can be learned as part of \mathbf{W} by adding 1 to the features of \mathbf{z}_n . Our loss function thus takes the following form $\mathcal{L}(\mathbf{W}) = \frac{1}{2} \|\mathbf{Y} - \mathbf{Z}\mathbf{W}\|_F^2$. To minimize this loss function, we will first find what matrices \mathbf{W} make the gradient of \mathcal{L} with respect to \mathbf{W} vanish. Hence, we need to find $\mathbf{W} \in \mathbb{R}^{K \times C}$ such that

$$\nabla_{\mathbf{W}} \mathcal{L} = \mathbf{0} \iff -\mathbf{Z}^T (\mathbf{Y} - \mathbf{Z}\mathbf{W}) = \mathbf{0} \iff \mathbf{Z}^T \mathbf{Y} = \mathbf{Z}^T \mathbf{Z}\mathbf{W}.$$

If we assumed \mathbf{Z} to be full rank, we would directly recover the usual least square solution $\mathbf{W}^* = (\mathbf{Z}^T \mathbf{Z})^{-1} \mathbf{Z}^T \mathbf{Y}$. However, we would like to (i) avoid any assumption on the spectrum of \mathbf{Z} , and (ii) avoid the use of any standard regularizer such as Tikhonov that is commonly used to recover a unique solution to an ill-posed optimization problem. In fact, our goal is to find the (possibly non-unique) family of parameters \mathbf{W}^* that fulfill $\nabla_{\mathbf{W}} \mathcal{L} = \mathbf{0}$ regardless of the properties of \mathbf{Z} and \mathbf{Y} . To that end, we first start by using the SVD of $\mathbf{Z} = \mathbf{U}_z \mathbf{\Sigma}_z \mathbf{V}_z^T$ —which always exists— to reformulate the above equality (see derivations in Appendices A.2 and A.3) into

$$\mathbf{Z}^T \mathbf{Y} = \mathbf{Z}^T \mathbf{Z}\mathbf{W} \iff \mathbf{W} \in \{(\mathbf{V}_z \mathbf{\Sigma}_z^{-1} \mathbf{U}_z^T + \bar{\mathbf{V}}_z \mathbf{M}) \mathbf{Y} : \mathbf{M} \in \mathbb{R}^{K \times C}\}, \quad (21)$$

with $\bar{\mathbf{V}}_z$ the $K \times (K - \text{rank}(\mathbf{Z}))$ matrix that horizontally stacks the right singular vectors of \mathbf{Z} which have their corresponding singular value 0, with the special case that $\mathbf{M} = \mathbf{0} \iff \text{rank}(\mathbf{Z}) = K$. We also slightly abuse notations and define $\mathbf{\Sigma}_z^{-1}$ to be the $K \times N$ matrix which is zero for all off-diagonal elements, and with

$$(\mathbf{\Sigma}_z^{-1})_{i,j} \triangleq \begin{cases} \frac{1}{(\sigma_z)_i} & \iff i = j \wedge (\sigma_z)_i > 0 \\ 0 & \text{otherwise} \end{cases},$$

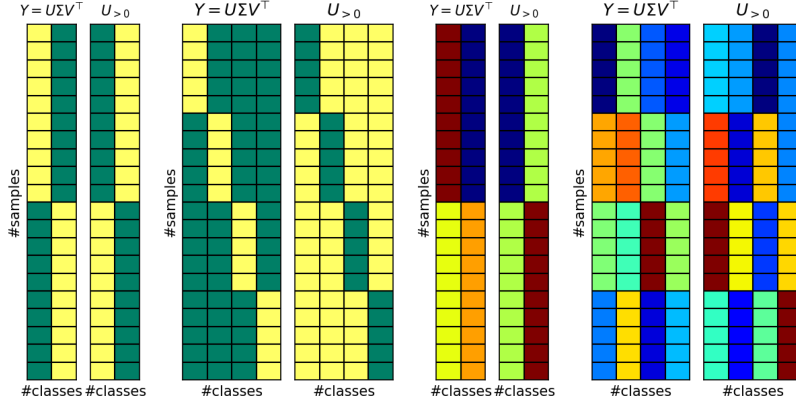


Figure 10: Depiction of typical target matrices \mathbf{Y} and their corresponding left singular vectors. Note that in this case all the nonzero singular values are identical, but with class-imbalance the singular values would be proportional to the class proportions. Hence it is clear that approximating the left singular vectors of \mathbf{Y} via SSL training (recall Theorem 9) the learned representations will exhibit per-class clustering—as long as the left-singular vectors of \mathbf{G} correctly encode the task.

hence $\Sigma_z^{-1}\Sigma_z$ is a $K \times K$ matrix which is identity iff \mathbf{X} is full rank, and is otherwise filled with $K - \text{rank}(\mathbf{X})$ zeros and $\text{rank}(\mathbf{X})$ ones in the diagonal. On the other hand, $\Sigma_z\Sigma_z^{-1}$ is a diagonal $N \times N$ matrix with $N - \text{rank}(\mathbf{X})$ zeros and $\text{rank}(\mathbf{X})$ ones in the diagonal. Note that in the special case where \mathbf{X} is full-rank, $\bar{\mathbf{V}}$ is null (we slightly abuse notations) and $\mathbf{V}_z\Sigma_z^{-1}\mathbf{U}_z^T = (\mathbf{Z}^T\mathbf{Z})^{-1}\mathbf{Z}^T$ recovering the standard least-square solution.

6.2 Necessary and Sufficient Conditions for Optimality of a Representation

Given a target matrix \mathbf{Y} and its SVD $\mathbf{U}_y\Sigma_y\mathbf{V}_y^T$, we obtain the following formal statement that demonstrates how the left-singular vectors of \mathbf{Y} must related to the left-singular vectors of \mathbf{Z} to allow for $\min_{\mathbf{W}} \mathcal{L}(\mathbf{W})$ to be 0. This statement plays a crucial role in our study as it answers the question *what property \mathbf{Z} must fulfill—regardless on how it was produced—to guarantee that 0 training error is achievable on the considered task?*

Theorem 8 (Necessary and sufficient condition). *Given a task $\mathbf{Y} \in \mathbb{R}^{N \times C}$ and a representation $\mathbf{Z} \in \mathbb{R}^{N \times K}$ —with left-singular vectors associated to nonzero singular values denoted as $\hat{\mathbf{U}}_z$ —the minimum linear loss is given by*

$$\min_{\mathbf{W} \in \mathbb{R}^{K \times C}} \mathcal{L}(\mathbf{W}) = \frac{1}{2} \|\mathbf{Y}\|_F^2 - \frac{1}{2} \|\hat{\mathbf{U}}_z^T \mathbf{U}_y \Sigma_y\|_F^2, \quad (22)$$

which is 0 iff the columns of $\hat{\mathbf{U}}_z$ spans the columns of $\hat{\mathbf{U}}_y$. (Proof in Appendix A.4.)

The proof consists in using the solution \mathbf{W} from the set in Eq. (21), and after a few algebraic manipulations, Theorem 9 result is obtained. From that result alone we already obtain an interesting requirement on \mathbf{Z} , namely that its top- K left singular vectors must be the same—up to a rotation—to the top- K left singular of \mathbf{Y} . Theorem 9 also provides us with a direct necessary condition but not sufficient condition for optimality.

Understanding the inter-play between $\text{rank}(\mathbf{Z})$, \mathbf{U}_z and \mathbf{U}_y will play a crucial role in the next section where we propose to study self-supervised learning criterion, and their ability to produce optimal representations.

6.3 Contrastive and Non-Contrastive Learning can all be Optimal

We now demonstrate in this section that any representation \mathbf{Z} learned by any of the SSL method (VICReg, BarlowTwins, SimCLR) can be optimal for a downstream task, as long as the data geometry encoded in \mathbf{G} follows the left-singular vectors of \mathbf{Y} , the target matrix which embodies the considered downstream task.

Theorem 9. *Given a dataset \mathbf{X} and relation matrix \mathbf{G} , minimizing the VICReg -or- SimCLR -or- BarlowTwins loss produces a representation that is optimal for a task $\mathbf{Y} = \mathbf{U}_y\Sigma_y\mathbf{V}_y^T$ iff the columns of $\hat{\mathbf{U}}_y$ are in the span of $\hat{\mathbf{U}}_g$ as in*

$$\min_{\mathbf{W} \in \mathbb{R}^{K \times C}} \|\mathbf{Y} - \mathbf{Z}^*\mathbf{W}\|_F^2 = 0 \iff \hat{\mathbf{U}}_y \in \text{span}(\hat{\mathbf{U}}_g),$$

with \mathbf{Z}^* the embeddings of the VICReg -or- SimCLR -or- BarlowTwins model after convergence. (Proof in Appendix A.17.)

Although not explicitly stated in Theorem 9 the same applies e.g. to NNCLR and MeanShift as they employ the same SimCLR loss, only the design of \mathbf{G} is altered. The above is crucial in helping and guiding the design of SSL methods and theoretically confirm the empirical findings from Geirhos et al. [2020] that observed in different scenarios that SSL and supervised models nearly fall back to the same thing.

6.4 Non-Contrastive Methods Should be Preferred: Best and Worst Downstream Task Error Bounds

We demonstrated in Section 6.3 that all SSL methods can be optimal to solve a task at hand as long as the spectral properties of \mathbf{G} and \mathbf{Y} are aligned. However, this is rarely the case in practical scenarios, and it thus becomes crucial to understand the behavior of the learned representation \mathbf{Z} on downstream task and if it varies with different SSL methods. First, we propose the following bound which represent the best and worst case downstream performances as a function of the rank of \mathbf{G} which is mostly a result of applying the Eckart-Young-Mirsky theorem. That is, we look at all the possible similarity matrices \mathbf{G} of rank R and see, given a task \mathbf{Y} what is the best achievable performance if \mathbf{G} correctly encodes the data geometry, and what is the worse possible performance if \mathbf{G} is “orthogonal” to the correct data geometry. For clarity and without loss of generality we assume here that $\text{rank}(\mathbf{Y}) \leq K$ as otherwise no method would produce an optimal representation in general and $K < N$ as otherwise we are in the kernel regime.

Theorem 10. *Given fixed inputs \mathbf{X} the lower and upper-bound over all possible matrices \mathbf{G} of rank R of the downstream task training performances (with fixed \mathbf{Y}) are given by*

$$\sum_{i=R}^K (\Sigma_{\mathbf{Y}}^2)_{i,i} \leq \left(\min_{\mathbf{W} \in \mathbb{R}^{K \times C}} \mathcal{L}(\mathbf{W}, \mathbf{Z}_{\text{SimCLR}}^*(\mathbf{G})) - \min_{\mathbf{W} \in \mathbb{R}^{K \times C}} \mathcal{L}(\mathbf{W}, \mathbf{Z}_{\text{VICReg}}^*(\mathbf{G})) \right) \leq \|\mathbf{Y}\|_F^2,$$

and are tight. Hence one should prefer VICReg, then BarlowTwins and finally SimCLR to maximize the downstream task performances.

The above result is a direct consequence of SimCLR forcing the representation to have the same rank as \mathbf{G} while VICReg always enforce a full-rank representation. And although this difference becomes irrelevant with correct \mathbf{G} (recall Section 6.3) it becomes an important distinctive attribute between SSL methods when \mathbf{G} is not optimal, which concerns most practical scenarios.

7 Conclusions

We provided in this study a unifying analysis of the major self-supervised learning methods covering VICReg (Section 3), SimCLR (Section 4) and BarlowTwins (Section 5). In doing so, we were able to not only tie each of those methods and their variants to common spectral embedding techniques, but we were also able to find the commonalities between all those methods. Among the many insights that we obtained, the most crucial one is that whenever the similarity matrix \mathbf{G} is correctly defined with respect to a downstream task, any of those methods will produce an ideal representation that will perfectly solve the task at hand. In short, there is no benefit of one method versus any other. In the more realistic regime where \mathbf{G} might be misaligned with the downstream task, VICReg with lower invariance regularization hyper-parameter should be preferred. In that regime, the representation will include all the information from \mathbf{G} while preserving full-rank and thus allowing for the representation to be usable for other downstream task that are not encoded within \mathbf{G} . This is in contrast with BarlowTwins and SimCLR that collapse the representation to embed all information about \mathbf{G} and nothing else.

At a more general level, we were able to parallel the contrastive versus non-contrastive dichotomy in SSL to the global versus local methods in spectral methods respectively. This led to further highlights into the strengths and weakness of each. For example, global approaches (contrastive SSL) tend to give a more faithful representation of the data’s global structure as the embedding aims to be metric-preserving. On the other hand, the local approaches (non-contrastive) provide useful embedding on a broader range of manifolds, whose local geometry is close to Euclidean, but whose global geometry may not be [Silva and Tenenbaum, 2002].

Beyond those results, we hope that the ties provided in this paper will stem a plurality of future work. One example would be to leverage the connection between SSL methods and spectral embedding methods to port existing results and techniques from one field to the other. In fact, such spectral methods have fallen short when dealing with high-dimensional datasets such as Imagenet. However, SSL methods have risen to become state-of-the-art on those datasets. The only difference between those lies in how \mathbf{G} is constructed.

Acknowledgements

We thank Prof. Pascal Vincent and Prof. Surya Ganguli for providing key discussions, insights and related work references that played a key role in making this study as complete and self-contained as possible.

References

- Nachman Aronszajn. Theory of reproducing kernels. *Transactions of the American mathematical society*, 68(3):337–404, 1950.
- Sanjeev Arora, Hrishikesh Khandeparkar, Mikhail Khodak, Orestis Plevrakis, and Nikunj Saunshi. A theoretical analysis of contrastive unsupervised representation learning. *arXiv preprint arXiv:1902.09229*, 2019.
- Alexei Baeovski, Yuhao Zhou, Abdelrahman Mohamed, and Michael Auli. wav2vec 2.0: A framework for self-supervised learning of speech representations. *Advances in Neural Information Processing Systems*, 33:12449–12460, 2020.
- Han Bao, Yoshihiro Nagano, and Kento Nozawa. Sharp learning bounds for contrastive unsupervised representation learning. *arXiv preprint arXiv:2110.02501*, 2021a.
- Hangbo Bao, Li Dong, and Furu Wei. Beit: Bert pre-training of image transformers. *arXiv preprint arXiv:2106.08254*, 2021b.
- Adrien Bardes, Jean Ponce, and Yann LeCun. Vicreg: Variance-invariance-covariance regularization for self-supervised learning. *arXiv preprint arXiv:2105.04906*, 2021.
- Maurice S Bartlett. Further aspects of the theory of multiple regression. In *Mathematical Proceedings of the Cambridge Philosophical Society*, volume 34, pages 33–40. Cambridge University Press, 1938.
- Mikhail Belkin and Partha Niyogi. Laplacian eigenmaps for dimensionality reduction and data representation. *Neural computation*, 15(6):1373–1396, 2003.
- Yoshua Bengio, Jean-françois Paiement, Pascal Vincent, Olivier Delalleau, Nicolas Roux, and Marie Ouimet. Out-of-sample extensions for lle, isomap, mds, eigenmaps, and spectral clustering. *Advances in neural information processing systems*, 16, 2003.
- Florian Bordes, Randall Balestriero, and Pascal Vincent. High fidelity visualization of what your self-supervised representation knows about. *arXiv preprint arXiv:2112.09164*, 2021.
- Roger W Brockett. Dynamical systems that sort lists, diagonalize matrices, and solve linear programming problems. *Linear Algebra and its applications*, 146:79–91, 1991.
- Jane Bromley, Isabelle Guyon, Yann LeCun, Eduard Säcker, and Roopak Shah. Signature verification using a " siamese" time delay neural network. *Advances in neural information processing systems*, 6, 1993.
- David S Broomhead and David Lowe. Radial basis functions, multi-variable functional interpolation and adaptive networks. Technical report, Royal Signals and Radar Establishment Malvern (United Kingdom), 1988.
- Mathilde Caron, Hugo Touvron, Ishan Misra, Hervé Jégou, Julien Mairal, Piotr Bojanowski, and Armand Joulin. Emerging properties in self-supervised vision transformers. In *Proceedings of the IEEE/CVF International Conference on Computer Vision*, pages 9650–9660, 2021.
- Ting Chen, Simon Kornblith, Mohammad Norouzi, and Geoffrey Hinton. A simple framework for contrastive learning of visual representations. In *International conference on machine learning*, pages 1597–1607. PMLR, 2020.
- Jian Cheng, Qingshan Liu, Hanqing Lu, and Yen-Wei Chen. Supervised kernel locality preserving projections for face recognition. *Neurocomputing*, 67:443–449, 2005.
- Patricia Cohen, Stephen G West, and Leona S Aiken. *Applied multiple regression/correlation analysis for the behavioral sciences*. Psychology press, 2014.
- John P Cunningham and Zoubin Ghahramani. Linear dimensionality reduction: Survey, insights, and generalizations. *The Journal of Machine Learning Research*, 16(1):2859–2900, 2015.
- Jacques Dauxois and Guy Martial Nkiet. Nonlinear canonical analysis and independence tests. *The Annals of Statistics*, 26(4):1254–1278, 1998.

- Xiaowen Dong, Dorina Thanou, Pascal Frossard, and Pierre Vandergheynst. Learning laplacian matrix in smooth graph signal representations. *IEEE Transactions on Signal Processing*, 64(23):6160–6173, 2016.
- Debidatta Dwibedi, Yusuf Aytar, Jonathan Tompson, Pierre Sermanet, and Andrew Zisserman. With a little help from my friends: Nearest-neighbor contrastive learning of visual representations. In *Proceedings of the IEEE/CVF International Conference on Computer Vision*, pages 9588–9597, 2021.
- Carl Eckart and Gale Young. The approximation of one matrix by another of lower rank. *Psychometrika*, 1(3): 211–218, 1936.
- Linus Ericsson, Henry Gouk, and Timothy M Hospedales. How well do self-supervised models transfer? In *Proceedings of the IEEE/CVF Conference on Computer Vision and Pattern Recognition*, pages 5414–5423, 2021.
- L Magnus Ewerbring and Franklin T Luk. Canonical correlations and generalized svd: applications and new algorithms. *Journal of computational and applied mathematics*, 27(1-2):37–52, 1989.
- Ronald A Fisher. The use of multiple measurements in taxonomic problems. *Annals of eugenics*, 7(2):179–188, 1936.
- Kenji Fukumizu, Francis R Bach, and Arthur Gretton. Statistical consistency of kernel canonical correlation analysis. *Journal of Machine Learning Research*, 8(2), 2007.
- Octavian Ganea, Sylvain Gelly, Gary Bécigneul, and Aliaksei Severyn. Breaking the softmax bottleneck via learnable monotonic pointwise non-linearities. In *International Conference on Machine Learning*, pages 2073–2082. PMLR, 2019.
- Robert Geirhos, Kantharaju Narayanappa, Benjamin Mitzkus, Matthias Bethge, Felix A Wichmann, and Wieland Brendel. On the surprising similarities between supervised and self-supervised models. *arXiv preprint arXiv:2010.08377*, 2020.
- Spyros Gidaris, Praveer Singh, and Nikos Komodakis. Unsupervised representation learning by predicting image rotations. *arXiv preprint arXiv:1803.07728*, 2018.
- Gene H Golub and Christian Reinsch. Singular value decomposition and least squares solutions. In *Linear algebra*, pages 134–151. Springer, 1971.
- Priya Goyal, Dhruv Mahajan, Abhinav Gupta, and Ishan Misra. Scaling and benchmarking self-supervised visual representation learning. In *Proceedings of the IEEE/CVF International Conference on Computer Vision*, pages 6391–6400, 2019.
- Arthur Gretton, Ralf Herbrich, Alexander Smola, Olivier Bousquet, Bernhard Schölkopf, et al. Kernel methods for measuring independence. 2005.
- Yue-Fei Guo, Shi-Jin Li, Jing-Yu Yang, Ting-Ting Shu, and Li-De Wu. A generalized foley–sammon transform based on generalized fisher discriminant criterion and its application to face recognition. *Pattern Recognition Letters*, 24(1-3):147–158, 2003.
- Raia Hadsell, Sumit Chopra, and Yann LeCun. Dimensionality reduction by learning an invariant mapping. In *2006 IEEE Computer Society Conference on Computer Vision and Pattern Recognition (CVPR’06)*, volume 2, pages 1735–1742. IEEE, 2006.
- Jeff Z HaoChen, Colin Wei, Adrien Gaidon, and Tengyu Ma. Provable guarantees for self-supervised deep learning with spectral contrastive loss. *Advances in Neural Information Processing Systems*, 34, 2021.
- Jeff Z HaoChen, Colin Wei, Ananya Kumar, and Tengyu Ma. Beyond separability: Analyzing the linear transferability of contrastive representations to related subpopulations. *arXiv preprint arXiv:2204.02683*, 2022.
- David R Hardoon, Sandor Szedmak, and John Shawe-Taylor. Canonical correlation analysis: An overview with application to learning methods. *Neural computation*, 16(12):2639–2664, 2004.
- Trevor Hastie, Andreas Buja, and Robert Tibshirani. Penalized discriminant analysis. *The Annals of Statistics*, 23(1):73–102, 1995.
- Ville Hautamaki, Ismo Karkkainen, and Pasi Franti. Outlier detection using k-nearest neighbour graph. In *Proceedings of the 17th International Conference on Pattern Recognition, 2004. ICPR 2004.*, volume 3, pages 430–433. IEEE, 2004.
- Kaiming He, Xinlei Chen, Saining Xie, Yanghao Li, Piotr Dollár, and Ross Girshick. Masked autoencoders are scalable vision learners. *arXiv preprint arXiv:2111.06377*, 2021.

- Xiaofei He and Partha Niyogi. Locality preserving projections. *Advances in neural information processing systems*, 16, 2003.
- MJR Healy. A rotation method for computing canonical correlations. *Mathematics of Computation*, 11(58): 83–86, 1957.
- Magnus R Hestenes. Inversion of matrices by biorthogonalization and related results. *Journal of the Society for Industrial and Applied Mathematics*, 6(1):51–90, 1958.
- Nicholas J Higham. Computing a nearest symmetric positive semidefinite matrix. *Linear algebra and its applications*, 103:103–118, 1988.
- Jorge E Hirsch. Discrete hubbard-stratonovich transformation for fermion lattice models. *Physical Review B*, 28(7):4059, 1983.
- Roger A Horn and Charles R Johnson. *Matrix analysis*. Cambridge university press, 2012.
- Tianyu Hua, Wenxiao Wang, Zihui Xue, Sucheng Ren, Yue Wang, and Hang Zhao. On feature decorrelation in self-supervised learning. In *Proceedings of the IEEE/CVF International Conference on Computer Vision*, pages 9598–9608, 2021.
- Carl J Huberty and Stephen Olejnik. *Applied MANOVA and discriminant analysis*. John Wiley & Sons, 2006.
- Like Hui and Mikhail Belkin. Evaluation of neural architectures trained with square loss vs cross-entropy in classification tasks, 2020. URL <https://arxiv.org/abs/2006.07322>.
- Sergey Ioffe. Probabilistic linear discriminant analysis. In *European Conference on Computer Vision*, pages 531–542. Springer, 2006.
- Li Jing, Pascal Vincent, Yann LeCun, and Yuandong Tian. Understanding dimensional collapse in contrastive self-supervised learning. *arXiv preprint arXiv:2110.09348*, 2021.
- Vassilis Kalofolias. How to learn a graph from smooth signals. In *Artificial Intelligence and Statistics*, pages 920–929. PMLR, 2016.
- Angjoo Kanazawa, David W Jacobs, and Manmohan Chandraker. WarpNet: Weakly supervised matching for single-view reconstruction. In *Proceedings of the IEEE Conference on Computer Vision and Pattern Recognition*, pages 3253–3261, 2016.
- Dahun Kim, Donghyeon Cho, and In So Kweon. Self-supervised video representation learning with space-time cubic puzzles. In *Proceedings of the AAAI conference on artificial intelligence*, volume 33, pages 8545–8552, 2019.
- H Knaf. Kernel fisher discriminant functions—a concise and rigorous introduction. 2007.
- Andrew V Knyazev. Convergence rate estimates for iterative methods for a mesh symmetric eigenvalue problem. 1987.
- Effrosini Kokiopoulou, Jie Chen, and Yousef Saad. Trace optimization and eigenproblems in dimension reduction methods. *Numerical Linear Algebra with Applications*, 18(3):565–602, 2011.
- Soroush Abbasi Koohpayegani, Ajinkya Tejankar, and Hamed Pirsiavash. Mean shift for self-supervised learning. In *Proceedings of the IEEE/CVF International Conference on Computer Vision*, pages 10326–10335, 2021.
- Joseph B Kruskal. Multidimensional scaling by optimizing goodness of fit to a nonmetric hypothesis. *Psychometrika*, 29(1):1–27, 1964.
- Olcay Kursun, Ethem Alpaydin, and Oleg V Favorov. Canonical correlation analysis using within-class coupling. *Pattern Recognition Letters*, 32(2):134–144, 2011.
- Malte Kuss and Thore Graepel. The geometry of kernel canonical correlation analysis. 2003.
- Pei Ling Lai and Colin Fyfe. Kernel and nonlinear canonical correlation analysis. *International Journal of Neural Systems*, 10(05):365–377, 2000.
- Cheng Li and Bingyu Wang. Fisher linear discriminant analysis. *CCIS Northeastern University*, 2014.
- Xin Liang, Ren-Cang Li, and Zhaojun Bai. Trace minimization principles for positive semi-definite pencils. *Linear Algebra and its Applications*, 438(7):3085–3106, 2013.
- Xin Liang, Li Wang, Lei-Hong Zhang, and Ren-Cang Li. On generalizing trace minimization. *arXiv preprint arXiv:2104.00257*, 2021.

- Sebastian Mika, Gunnar Ratsch, Jason Weston, Bernhard Scholkopf, and Klaus-Robert Mullers. Fisher discriminant analysis with kernels. In *Neural networks for signal processing IX: Proceedings of the 1999 IEEE signal processing society workshop (cat. no. 98th8468)*, pages 41–48. Ieee, 1999.
- Ishan Misra and Laurens van der Maaten. Self-supervised learning of pretext-invariant representations. In *Proceedings of the IEEE/CVF Conference on Computer Vision and Pattern Recognition*, pages 6707–6717, 2020.
- Azade Nazi, Will Hang, Anna Goldie, Sujith Ravi, and Azalia Mirhoseini. Generalized clustering by learning to optimize expected normalized cuts. *arXiv preprint arXiv:1910.07623*, 2019.
- David Novotny, Samuel Albanie, Diane Larlus, and Andrea Vedaldi. Self-supervised learning of geometrically stable features through probabilistic introspection. In *Proceedings of the IEEE Conference on Computer Vision and Pattern Recognition*, pages 3637–3645, 2018.
- Ralph G O’Brien and Mary K Kaiser. Manova method for analyzing repeated measures designs: an extensive primer. *Psychological bulletin*, 97(2):316, 1985.
- David Pfau, Stig Petersen, Ashish Agarwal, David G. T. Barrett, and Kimberly L. Stachenfeld. Spectral inference networks: Unifying deep and spectral learning. In *International Conference on Learning Representations*, 2019. URL <https://openreview.net/forum?id=SJzqpj09YQ>.
- Ashwini Pogle, Jinjin Tian, Yuchen Li, and Andrej Risteski. Contrasting the landscape of contrastive and non-contrastive learning. *arXiv preprint arXiv:2203.15702*, 2022.
- Franco P Preparata and Michael I Shamos. *Computational geometry: an introduction*. Springer Science & Business Media, 2012.
- Jiezhong Qiu, Yuxiao Dong, Hao Ma, Jian Li, Kuansan Wang, and Jie Tang. Network embedding as matrix factorization: Unifying deepwalk, line, pte, and node2vec. In *Proceedings of the eleventh ACM international conference on web search and data mining*, pages 459–467, 2018.
- Sam T Roweis and Lawrence K Saul. Nonlinear dimensionality reduction by locally linear embedding. *science*, 290(5500):2323–2326, 2000.
- Bernhard Schölkopf, Alexander Smola, and Klaus-Robert Müller. Nonlinear component analysis as a kernel eigenvalue problem. *Neural computation*, 10(5):1299–1319, 1998.
- Pierre Sermanet, Corey Lynch, Yevgen Chebotar, Jasmine Hsu, Eric Jang, Stefan Schaal, Sergey Levine, and Google Brain. Time-contrastive networks: Self-supervised learning from video. In *2018 IEEE international conference on robotics and automation (ICRA)*, pages 1134–1141. IEEE, 2018.
- Haizhou Shi, Dongliang Luo, Siliang Tang, Jian Wang, and Yueting Zhuang. Run away from your teacher: Understanding byol by a novel self-supervised approach. *arXiv preprint arXiv:2011.10944*, 2020.
- Vin Silva and Joshua Tenenbaum. Global versus local methods in nonlinear dimensionality reduction. *Advances in neural information processing systems*, 15, 2002.
- Donald F Specht et al. A general regression neural network. *IEEE transactions on neural networks*, 2(6): 568–576, 1991.
- Henning Sprekeler. On the relation of slow feature analysis and laplacian eigenmaps. *Neural computation*, 23(12):3287–3302, 2011.
- Mariko Tai, Mineichi Kudo, Akira Tanaka, Hideyuki Imai, and Keigo Kimura. Kernelized supervised laplacian eigenmap for visualization and classification of multi-label data. *Pattern Recognition*, 123:108399, 2022.
- Joshua B Tenenbaum, Vin de Silva, and John C Langford. A global geometric framework for nonlinear dimensionality reduction. *science*, 290(5500):2319–2323, 2000.
- Yuangong Tian. Deep contrastive learning is provably (almost) principal component analysis. *arXiv preprint arXiv:2201.12680*, 2022.
- Yuangong Tian, Xinlei Chen, and Surya Ganguli. Understanding self-supervised learning dynamics without contrastive pairs. In *International Conference on Machine Learning*, pages 10268–10278. PMLR, 2021.
- Christopher Tosh, Akshay Krishnamurthy, and Daniel Hsu. Contrastive learning, multi-view redundancy, and linear models. In *Algorithmic Learning Theory*, pages 1179–1206. PMLR, 2021.
- Viivi Uurtio, João M Monteiro, Jaz Kandola, John Shawe-Taylor, Delmiro Fernandez-Reyes, and Juho Rousu. A tutorial on canonical correlation methods. *ACM Computing Surveys (CSUR)*, 50(6):1–33, 2017.
- Hrishikesh D Vinod. Canonical ridge and econometrics of joint production. *Journal of econometrics*, 4(2): 147–166, 1976.

- Ulrike Von Luxburg. A tutorial on spectral clustering. *Statistics and computing*, 17(4):395–416, 2007.
- Huan Wang, Shuicheng Yan, Dong Xu, Xiaoou Tang, and Thomas Huang. Trace ratio vs. ratio trace for dimensionality reduction. In *2007 IEEE Conference on Computer Vision and Pattern Recognition*, pages 1–8. IEEE, 2007.
- Tongzhou Wang and Phillip Isola. Understanding contrastive representation learning through alignment and uniformity on the hypersphere. In *International Conference on Machine Learning*, pages 9929–9939. PMLR, 2020.
- Xiang Wang, Xinlei Chen, Simon S Du, and Yuandong Tian. Towards demystifying representation learning with non-contrastive self-supervision. *arXiv preprint arXiv:2110.04947*, 2021.
- Andrew J Wathen and Shengxin Zhu. On spectral distribution of kernel matrices related to radial basis functions. *Numerical Algorithms*, 70(4):709–726, 2015.
- Andrew R Webb. Multidimensional scaling by iterative majorization using radial basis functions. *Pattern Recognition*, 28(5):753–759, 1995.
- Andrew R Webb. *Statistical pattern recognition*. John Wiley & Sons, 2003.
- Kilian Q Weinberger and Lawrence K Saul. Distance metric learning for large margin nearest neighbor classification. *Journal of machine learning research*, 10(2), 2009.
- Zixin Wen and Yuanzhi Li. Toward understanding the feature learning process of self-supervised contrastive learning. In *International Conference on Machine Learning*, pages 11112–11122. PMLR, 2021.
- Christopher Williams. On a connection between kernel pca and metric multidimensional scaling. *Advances in neural information processing systems*, 13, 2000.
- Daniela M Witten, Robert Tibshirani, and Trevor Hastie. A penalized matrix decomposition, with applications to sparse principal components and canonical correlation analysis. *Biostatistics*, 10(3):515–534, 2009.
- Eric Xing, Michael Jordan, Stuart J Russell, and Andrew Ng. Distance metric learning with application to clustering with side-information. *Advances in neural information processing systems*, 15, 2002.
- Dejing Xu, Jun Xiao, Zhou Zhao, Jian Shao, Di Xie, and Yueting Zhuang. Self-supervised spatiotemporal learning via video clip order prediction. In *Proceedings of the IEEE/CVF Conference on Computer Vision and Pattern Recognition*, pages 10334–10343, 2019.
- Jing-Hao Xue and Peter Hall. Why does rebalancing class-unbalanced data improve auc for linear discriminant analysis? *IEEE transactions on pattern analysis and machine intelligence*, 37(5):1109–1112, 2014.
- Zhilin Yang, Zihang Dai, Ruslan Salakhutdinov, and William W Cohen. Breaking the softmax bottleneck: A high-rank rnn language model. *arXiv preprint arXiv:1711.03953*, 2017.
- Jure Zbontar, Li Jing, Ishan Misra, Yann LeCun, and Stéphane Deny. Barlow twins: Self-supervised learning via redundancy reduction. *arXiv preprint arXiv:2103.03230*, 2021.

Supplementary Materials

The supplementary materials is providing the proofs of the main's paper formal results. We also provide as much background results and references as possible throughout to ensure that all the derivations are self-contained. Some of the below derivation do not belong to formal statements but are included to help the curious readers get additional insights into current SSL methods.

A Formal Statements Proofs

A.1 VICReg Variance+Covariance Versus Representation's Singular Values

This simple derivation demonstrates how minimizing the VCREg can be done through an upper bound by constraining all the singular-values to be close to 1 although the general criterion only enforces for the variance term to be —at least— 1 through the following derivations

$$\begin{aligned}
 \min_{\mathbf{Z}} \min_{\mathbf{u} \in [1, \infty)^\kappa} \|\mathbf{Z}^T \mathbf{Z} - \text{diag}(\mathbf{u})\|_F^2 &= \min_{\mathbf{Z}} \min_{\mathbf{u} \in [1, \infty)^\kappa} \|\mathbf{V}_Z \Sigma_Z^2 \mathbf{V}_Z^T - \text{diag}(\mathbf{u})\|_F^2 \\
 &= \min_{\mathbf{Z}} \min_{\mathbf{u} \in [1, \infty)^\kappa} \|\Sigma_Z^2 - \text{diag}(\mathbf{u})\|_F^2 \\
 &= \min_{\mathbf{Z}} \min_{\mathbf{u} \in [1, \infty)^\kappa} \|\sigma_Z^2 - \mathbf{u}\|_2^2 \\
 &\leq \min_{\mathbf{Z}} \|\sigma_Z^2 - \mathbf{1}\|_2^2
 \end{aligned}$$

where we denoted by σ_Z the diagonal part of the diagonal Σ_Z matrix.

A.2 Non-Unique Solution to Least-Square

The below derivation demonstrates that even in the representation \mathbf{Z} (or any input matrix) is not full-rank, the least-square type of solution \mathbf{W} to predict $\mathbf{Y} = \mathbf{Z}\mathbf{W}$ can be found, it is just not unique. In fact, it is possible to find an entire space of matrices that will minimize the loss i.e. respect the below equality that makes the loss have a gradient of 0 and be at its minimum value, simply by moving within the kernel space of the representation (input) matrix as in

$$\begin{aligned}
 \mathbf{Z}^T \mathbf{Y} = \mathbf{Z}^T \mathbf{Z} \mathbf{W} &\iff (\mathbf{U}_Z \Sigma_Z \mathbf{V}_Z^T)^T \mathbf{Y} = (\mathbf{U}_Z \Sigma_Z \mathbf{V}_Z^T)^T (\mathbf{U}_Z \Sigma_Z \mathbf{V}_Z^T) \mathbf{W} \\
 &\iff \mathbf{V}_Z \Sigma_Z^T \mathbf{U}_Z^T \mathbf{Y} = \mathbf{V}_Z \Sigma_Z^T \Sigma_Z \mathbf{V}_Z^T \mathbf{W} \\
 &\iff \mathbf{W}^* \in \{(\mathbf{V}_Z \Sigma_Z^{-1} \mathbf{U}_Z^T + \mathbf{M}) \mathbf{Y} : \mathbf{M} \in \ker(\mathbf{Z})\},
 \end{aligned}$$

where we recall that $\ker(\mathbf{Z})$ is the kernel space of \mathbf{Z} , and where we slightly abused notations by employing Σ_Z^{-1} to represent the inverse only for the non-zero element of the diagonal matrix Σ_Z (there are as many zeros in the diagonal as the dimension of $\ker(\mathbf{Z})$).

A.3 Any Linear Weight from Appendix A.2 Has Zero Least-Square Gradient

This section continues the previous derivations but now demonstrating that using this optimal value for \mathbf{W} denoted as \mathbf{W}^* does fulfill the equality i.e. we are at a global optimum for any matrix within the defined subspace as in

$$\begin{aligned}
 \mathbf{V}_Z \Sigma_Z^T \mathbf{U}_Z^T \mathbf{Y} &= \mathbf{V}_Z \Sigma_Z^T \Sigma_Z \mathbf{V}_Z^T \mathbf{W}^* \\
 \implies \mathbf{V}_Z \Sigma_Z^T \mathbf{U}_Z^T \mathbf{Y} &= \mathbf{V}_Z \Sigma_Z^T \Sigma_Z \mathbf{V}_Z^T (\mathbf{V}_Z \Sigma_Z^{-1} \mathbf{U}_Z^T + \mathbf{M}) \mathbf{Y} \\
 \implies \mathbf{V}_Z \Sigma_Z^T \mathbf{U}_Z^T \mathbf{Y} &= \mathbf{V}_Z \Sigma_Z^T \Sigma_Z \Sigma_Z^{-1} \mathbf{U}_Z^T \mathbf{Y} \\
 \implies \mathbf{V}_Z \Sigma_Z^T \mathbf{U}_Z^T \mathbf{Y} &= \mathbf{V}_Z \text{diag}(\sigma_Z)^2 \Sigma_Z^{-1} \mathbf{U}_Z^T \mathbf{Y} \\
 \implies \mathbf{V}_Z \Sigma_Z^T \mathbf{U}_Z^T \mathbf{Y} &= \mathbf{V}_Z \Sigma_Z^T \mathbf{U}_Z^T \mathbf{Y}
 \end{aligned}$$

where the last equality follows since $\text{diag}(\sigma_Z)^2 \Sigma_Z^{-1}$ will either multiply $(\sigma_Z)_i^2$ with $(\Sigma_Z^{-1})_{i,i} = \frac{1}{(\sigma_Z)_i}$ if $(\sigma_Z)_i$ is nonzero, and otherwise if $(\sigma_Z)_i$ is 0, then it will be the product between 0 for $(\sigma_Z)_i^2$ and 0 for $(\Sigma_Z^{-1})_{i,i}$ giving back the original value for $(\sigma_Z)_i$.

A.4 Achievable Loss with Low-Rank Representation

This section takes a last detour towards understanding the least-square loss with a low-rank input/representation matrix. In this case we derive a various set of quantities that quantify the minimum loss that is achieved by any of the optimal matrix \mathbf{W}^* found in Appendix A.2 as follows again slightly abusing notations for $\Sigma_{\mathbf{Z}}^{-1}$ to only invert the non-zero singular values of \mathbf{Z} as

$$\begin{aligned}
\frac{1}{2}\|\mathbf{Y} - \mathbf{Z}\mathbf{W}^*\|_F^2 &= \frac{1}{2}\|\mathbf{Y} - \mathbf{Z}(\mathbf{V}_{\mathbf{Z}}\Sigma_{\mathbf{Z}}^{-1}\mathbf{U}_{\mathbf{Z}}^T + \tilde{\mathbf{V}}_{\mathbf{Z}}\mathbf{M})\mathbf{Y}\|_F^2 \\
&= \frac{1}{2}\|\mathbf{Y} - \mathbf{U}_{\mathbf{Z}}\Sigma_{\mathbf{Z}}\mathbf{V}_{\mathbf{Z}}^T\mathbf{V}_{\mathbf{Z}}\Sigma_{\mathbf{Z}}^{-1}\mathbf{U}_{\mathbf{Z}}^T\mathbf{Y}\|_F^2 \\
&= \frac{1}{2}\|\mathbf{Y} - \mathbf{U}_{\mathbf{Z}}\Sigma_{\mathbf{Z}}\Sigma_{\mathbf{Z}}^{-1}\mathbf{U}_{\mathbf{Z}}^T\mathbf{Y}\|_F^2 \\
&= \frac{1}{2}\|(\mathbf{I} - \mathbf{U}_{\mathbf{Z}}\Sigma_{\mathbf{Z}}\Sigma_{\mathbf{Z}}^{-1}\mathbf{U}_{\mathbf{Z}}^T)\mathbf{Y}\|_F^2 \\
&= \frac{1}{2}\|(\mathbf{U}_{\mathbf{Z}}\mathbf{U}_{\mathbf{Z}}^T - \mathbf{U}_{\mathbf{Z}}\Sigma_{\mathbf{Z}}\Sigma_{\mathbf{Z}}^{-1}\mathbf{U}_{\mathbf{Z}}^T)\mathbf{Y}\|_F^2 \\
&= \frac{1}{2}\|(\mathbf{I} - \Sigma_{\mathbf{Z}}\Sigma_{\mathbf{Z}}^{-1})\mathbf{U}_{\mathbf{Z}}^T\mathbf{Y}\|_F^2 \\
&= \frac{1}{2}\|\mathbf{Y}\|_F^2 - \frac{1}{2}\|\Sigma_{\mathbf{Z}}\Sigma_{\mathbf{Z}}^{-1}\mathbf{U}_{\mathbf{Z}}^T\mathbf{Y}\|_F^2 \\
&= \frac{1}{2}\|\mathbf{Y}\|_F^2 - \frac{1}{2}\|\Sigma_{\mathbf{Z}}\Sigma_{\mathbf{Z}}^{-1}\mathbf{U}_{\mathbf{Z}}^T\mathbf{U}_y\Sigma_y\|_F^2 \\
&= \frac{1}{2}\|\mathbf{Y}\|_F^2 - \frac{1}{2}\sum_{i,j}1_{\{(\sigma_{\mathbf{Z}})_i>0\}}\langle(\mathbf{U}_{\mathbf{Z}})_i, (\mathbf{U}_y)_j\rangle^2(\sigma_y)_j^2,
\end{aligned}$$

where it is clear that the minimum loss will in general not be 0 unless $\Sigma_{\mathbf{Z}}\Sigma_{\mathbf{Z}}^{-1} = \mathbf{I}$ which is not guaranteed (recall that we abuse notation for the inverse and that $\Sigma_{\mathbf{Z}}\Sigma_{\mathbf{Z}}^{-1}$ is only 1 in its diagonal for the nonzero singular values of \mathbf{Z}).

A.5 Equivalence Between VICReg Invariance Term and Trace with Graph Laplacian

The goal of this section is to derive the first crucial result of our study that ties VICReg to spectral embedding methods by doing a first connection between VICReg invariance loss and the Dirichlet energy of a graph. The equality follows from the Laplacian of the graph definition $\mathbf{L} = \mathbf{D} - \mathbf{G}$ where \mathbf{D} is the degree matrix of the graph i.e. a diagonal matrix with entries corresponding to the sum of each row of \mathbf{G} , and using the following algebraic manipulations which are common in the spectral graph analysis community, see e.g. [Von Luxburg, 2007]

$$\begin{aligned}
\text{Tr}(\mathbf{Z}^T\mathbf{L}\mathbf{Z}) &= \sum_d(\mathbf{Z}^T\mathbf{L}\mathbf{Z})_{d,d} = \sum_{i,j}\mathbf{L}_{i,j}\langle(\mathbf{Z})_{j,\cdot}, (\mathbf{Z})_{i,\cdot}\rangle \\
&= \sum_i\|(\mathbf{Z})_{i,\cdot}\|_2^2(\mathbf{D})_{i,i} - \sum_{i,j}(\mathbf{G})_{i,j}\langle(\mathbf{Z})_{j,\cdot}, (\mathbf{Z})_{i,\cdot}\rangle \\
&= \frac{\sum_i\|(\mathbf{Z})_{i,\cdot}\|_2^2(\mathbf{D})_{i,i} + \sum_i\|(\mathbf{Z})_{i,\cdot}\|_2^2(\mathbf{D})_{i,i}}{2} - \sum_{i,j}(\mathbf{G})_{i,j}\langle(\mathbf{Z})_{j,\cdot}, (\mathbf{Z})_{i,\cdot}\rangle \\
&= \frac{\sum_i\sum_j\|(\mathbf{Z})_{i,\cdot}\|_2^2(\mathbf{G})_{i,j} + \sum_i\sum_j\|(\mathbf{Z})_{i,\cdot}\|_2^2(\mathbf{G})_{i,j}}{2} - \sum_{i,j}(\mathbf{G})_{i,j}\langle(\mathbf{Z})_{j,\cdot}, (\mathbf{Z})_{i,\cdot}\rangle \\
&= \frac{1}{2}\sum_i\sum_j(\mathbf{G})_{i,j}\|(\mathbf{Z})_{i,\cdot} - (\mathbf{Z})_{j,\cdot}\|_2^2,
\end{aligned}$$

which is a famous derivation in graph signal processing relating pairwise distances to Dirichlet energy of the underlying graph with Laplacian \mathbf{L} .

A.6 Non-Uniqueness of a Representation to a Given VICReg Loss Value

In this section we provide a simple argument to demonstrate that the VICReg representation that obtains a loss value of c is not unique, regardless of the (achievable) value of c . To see that, one can for example add a constant vector to each row of \mathbf{Z} and see that Eq. (2) is left unchanged. In fact the computation of the covariance matrix is invariant to constant column shift of \mathbf{Z} , and the invariance term will automatically cancel those added vectors when comparing pairs of rows.

A.7 Optimal Representation and Loss for VICReg (Theorem 1)

The goal of this section is to obtain the closed-form optimal representation of VICReg using the least-square variance loss, instead of the hinge-loss, and to find the minimum loss associated to that (non-unique) optimum. Using the Trace term derivations given in Appendix A.5 we obtain

$$\mathcal{L}_{\text{VIC}} = \alpha \|\text{Cov}(\mathbf{Z}_{\alpha,\gamma}^*) - \mathbf{I}\|_F^2 + 2\frac{\gamma}{N} \text{Tr} \left((\mathbf{P}'_{\alpha,\gamma} (\boldsymbol{\Lambda}'_{\alpha,\gamma} N)^{1/2})^T \mathbf{L} \mathbf{P}'_{\alpha,\gamma} (\boldsymbol{\Lambda}'_{\alpha,\gamma} N)^{1/2} \right),$$

where we use $\boldsymbol{\lambda}'_{\alpha,\beta}$, $\mathbf{P}'_{\alpha,\gamma}$ and $\boldsymbol{\Lambda}'_{\alpha,\gamma}$ to denote the first K indices/columns of Eq. (8). Simplifying the trace term leads to

$$\begin{aligned} \frac{\gamma}{N} \text{Tr} \left((\mathbf{P}'_{\alpha,\gamma} (\boldsymbol{\Lambda}'_{\alpha,\gamma} N)^{1/2})^T \mathbf{L} \mathbf{P}'_{\alpha,\gamma} (\boldsymbol{\Lambda}'_{\alpha,\gamma} N)^{1/2} \right) &= \gamma \text{Tr} \left(\boldsymbol{\Lambda}'_{\alpha,\gamma} \mathbf{P}'_{\alpha,\gamma}{}^T \mathbf{L} \mathbf{P}'_{\alpha,\gamma} \right) \\ &= \alpha \text{Tr} \left(\boldsymbol{\Lambda}'_{\alpha,\gamma} \mathbf{P}'_{\alpha,\gamma}{}^T \mathbf{M} \mathbf{P}'_{\alpha,\gamma} \right) \\ &\quad - \alpha \text{Tr} \left(\boldsymbol{\Lambda}'_{\alpha,\gamma} \mathbf{P}'_{\alpha,\gamma}{}^T (\mathbf{M} - \frac{\gamma}{\alpha} \mathbf{L}) \mathbf{P}'_{\alpha,\gamma} \right) \\ &= \alpha \text{Tr} \left(\boldsymbol{\Lambda}'_{\alpha,\gamma} \mathbf{P}'_{\alpha,\gamma}{}^T (\mathbf{I} - \frac{1}{N} \mathbf{1}\mathbf{1}^T) \mathbf{P}'_{\alpha,\gamma} \right) - \alpha \|\boldsymbol{\lambda}'_{\alpha,\gamma}\|_2^2, \end{aligned}$$

plugging this value into the loss we obtain

$$\begin{aligned} \mathcal{L}_{\text{VIC}} &= \alpha \left(\|\text{Cov}(\mathbf{Z}_{\alpha,\gamma}^*) - \mathbf{I}\|_F^2 + 2 \text{Tr} \left(\boldsymbol{\Lambda}'_{\alpha,\gamma} \mathbf{P}'_{\alpha,\gamma}{}^T (\mathbf{I} - \frac{1}{N} \mathbf{1}\mathbf{1}^T) \mathbf{P}'_{\alpha,\gamma} \right) - 2 \|\boldsymbol{\lambda}'_{\alpha,\gamma}\|_2^2 \right) \\ &= \alpha \left(\|\text{Cov}(\mathbf{Z}_{\alpha,\gamma}^*)\|_F^2 + K - 2 \text{Tr}(\text{Cov}(\mathbf{Z}_{\alpha,\gamma}^*)) + 2 \text{Tr} \left(\boldsymbol{\Lambda}'_{\alpha,\gamma} \mathbf{P}'_{\alpha,\gamma}{}^T (\mathbf{I} - \frac{1}{N} \mathbf{1}\mathbf{1}^T) \mathbf{P}'_{\alpha,\gamma} \right) - 2 \|\boldsymbol{\lambda}'_{\alpha,\gamma}\|_2^2 \right) \\ &= \alpha \left(\|\text{Cov}(\mathbf{Z}_{\alpha,\gamma}^*)\|_F^2 + K - 2 \|\boldsymbol{\lambda}'_{\alpha,\gamma}\|_2^2 \right) \\ &= \alpha \left(\left\| \frac{1}{N} (\mathbf{Z}_{\alpha,\gamma}^*)^T \mathbf{M} \mathbf{Z}_{\alpha,\gamma}^* \right\|_F^2 + K - 2 \|\boldsymbol{\lambda}'_{\alpha,\gamma}\|_2^2 \right), \end{aligned}$$

now one should recall that $\mathbf{Z}_{\alpha,\gamma}^*$ contains the eigenvectors of $\mathbf{M} - \frac{\gamma}{\alpha} \mathbf{L}$ and that each of those eigenvector that has nonzero singular value has 0 mean since

$$\begin{aligned} (\mathbf{M} - \frac{\gamma}{\alpha} \mathbf{L}) \mathbf{v} &= \lambda \mathbf{v} \\ \iff \mathbf{M} (\mathbf{I} - \frac{\gamma}{\alpha} \mathbf{L}) \mathbf{M} \mathbf{v} &= \lambda \mathbf{v} && \text{(Laplacian rows/cols sum to 0)} \\ \implies \mathbf{1}^T \mathbf{M} (\mathbf{I} - \frac{\gamma}{\alpha} \mathbf{L}) \mathbf{M} \mathbf{v} &= \lambda \mathbf{1}^T \mathbf{v} \\ \implies 0 = \lambda \mathbf{1}^T \mathbf{v} &\implies \mathbf{1}^T \mathbf{v} = 0 && \text{(for any eigenvector } \mathbf{v} \text{ with } \lambda > 0) \end{aligned}$$

hence we obtain the following simplifications

$$\begin{aligned} \mathcal{L}_{\text{VIC}} &= \alpha \left(\left\| \frac{1}{N} (\mathbf{Z}_{\alpha,\gamma}^*)^T \mathbf{M} \mathbf{Z}_{\alpha,\gamma}^* \right\|_F^2 + K - 2 \|\boldsymbol{\lambda}'_{\alpha,\gamma}\|_2^2 \right) \\ &= \alpha \left(\left\| \frac{1}{N} (\mathbf{Z}_{\alpha,\gamma}^*)^T \mathbf{Z}_{\alpha,\gamma}^* \right\|_F^2 + K - 2 \|\boldsymbol{\lambda}'_{\alpha,\gamma}\|_2^2 \right) \\ &= \alpha \left(\|\boldsymbol{\lambda}'_{\alpha,\gamma}\|_2^2 + K - 2 \|\boldsymbol{\lambda}'_{\alpha,\gamma}\|_2^2 \right) \\ &= \alpha (K - \|\boldsymbol{\lambda}'_{\alpha,\gamma}\|_2^2) \end{aligned}$$

which concludes the proof.

A.8 Proof of VICReg Recovering Laplacian Eigenmaps (Theorem 2)

This section takes on proving the first key result of our study that thoroughly tie VICReg to the known local spectral embedding method Laplacian Eigenmap. The only difference would be that in our case the graph \mathbf{G} is given from an SSL viewpoint and not constructed from a k-NN graph and geodesic distance estimate as in LE. We already know from Appendix A.5 that the invariance term of VICReg corresponds to the Trace term (times 2) that LE tries to minimize. The only thing that we have to show to have the equivalent between the two is that the constraint $\mathbf{Z}^T \mathbf{D} \mathbf{Z} = \mathbf{I}$ is equivalent to the one that imposes an exact minimization of the variance and covariance terms. To see that, first notice (or recall from Appendix A.7) that the variance+covariance term can be expressed as $\|\frac{1}{N} \mathbf{Z}^T \mathbf{M} \mathbf{Z} - \mathbf{I}\|_F^2$. Now, recall that the minimizer of LE consists in taking the $[2 : K + 1]$ eigenvectors of the Laplacian matrix $\mathbf{I} - \mathbf{D}^{-1} \mathbf{G}$ which is equivalent (up to a rescaling of the eigenvalues) to taking the eigenvectors of $\mathbf{D} - \mathbf{G}$ as long as \mathbf{D} is isotropic. We also already saw that those eigenvectors either have zero mean and nonzero eigenvalue, or have arbitrary means and zero eigenvalue. As LE only considers the eigenvectors with nonzero eigenvalues, it is direct to see that those eigenvectors are centered. This translates to $\|\frac{1}{N} \mathbf{Z}^T \mathbf{M} \mathbf{Z} - \mathbf{I}\|_F^2 = \|\frac{1}{N} \mathbf{Z}^T \mathbf{Z} - \mathbf{I}\|_F^2$. Hence, up to a rescaling, as long as \mathbf{D} is isotropic ($\mathbf{D} = c\mathbf{I}$) which is always the case in SSL, enforcing $\mathcal{L}_{\text{var}} = 0, \text{cov} = 0$ is equivalent to $\mathbf{Z}^T \mathbf{Z} = \frac{N}{c} \mathbf{I}$.

A.9 Proof of Linear VICReg Optimal Parameters (Eq. (12))

We are again using the quadratic variance term in-place of the hinge-term at 1. In that setting, the linear VICReg loss falls back to

$$\mathcal{L}_{\text{vic}} = \alpha \left\| \frac{1}{N} \mathbf{W}^T \mathbf{X}^T \mathbf{H} \mathbf{X} \mathbf{W} - \mathbf{I} \right\|_F^2 + \frac{2\gamma}{N} \text{Tr}(\mathbf{W}^T \mathbf{X}^T \mathbf{L} \mathbf{X} \mathbf{W}),$$

which can be written in term of traces only to simplify differentiation as

$$\begin{aligned} \mathcal{L}_{\text{vic}} &= \frac{\alpha}{N^2} \text{Tr}(\mathbf{W}^T \mathbf{X}^T \mathbf{H} \mathbf{X} \mathbf{W} \mathbf{W}^T \mathbf{X}^T \mathbf{H} \mathbf{X} \mathbf{W}) \\ &\quad - \frac{2\alpha}{N} \text{Tr}(\mathbf{W}^T \mathbf{X}^T \mathbf{H} \mathbf{X} \mathbf{W}) + \frac{2\gamma}{N} \text{Tr}(\mathbf{W}^T \mathbf{X}^T \mathbf{L} \mathbf{X} \mathbf{W}) + \text{cst} \\ &= \frac{\alpha}{N^2} \text{Tr}(\mathbf{W}^T \mathbf{X}^T \mathbf{H} \mathbf{X} \mathbf{W} \mathbf{W}^T \mathbf{X}^T \mathbf{H} \mathbf{X} \mathbf{W}) + \frac{2}{N} \text{Tr}(\mathbf{W}^T \mathbf{X}^T (\gamma \mathbf{L} - \alpha \mathbf{H}) \mathbf{X} \mathbf{W}) + \text{cst} \end{aligned}$$

which we can now differentiate with respect to the \mathbf{W} parameter to obtain

$$\nabla_{\mathbf{W}} \mathcal{L}_{\text{vic}} = \frac{4\alpha}{N^2} \mathbf{X}^T \mathbf{H} \mathbf{X} \mathbf{W} \mathbf{W}^T \mathbf{X}^T \mathbf{H} \mathbf{X} \mathbf{W} + \frac{4}{N} \mathbf{X}^T (\gamma \mathbf{L} - \alpha \mathbf{H}) \mathbf{X} \mathbf{W},$$

which we need to set to 0 and thus can be simplified to (since $\alpha > 0$)

$$\nabla_{\mathbf{W}} \mathcal{L}_{\text{vic}} = \frac{1}{N} \mathbf{X}^T \mathbf{H} \mathbf{X} \mathbf{W} \mathbf{W}^T \mathbf{X}^T \mathbf{H} \mathbf{X} \mathbf{W} + \mathbf{X}^T \left(\frac{\gamma}{\alpha} \mathbf{L} - \mathbf{H} \right) \mathbf{X} \mathbf{W}.$$

First, let's consider that $\mathbf{X}^T \mathbf{H} \mathbf{X}$ is invertible i.e. the data lies on a D -dimensional affine space. If not, the original data \mathbf{X} can simply be projected onto its subspace prior applying VICReg. In that setting and if $K = D$, we directly obtain

$$\begin{aligned} \nabla_{\mathbf{W}} \mathcal{L}_{\text{vic}} &= \mathbf{0} \\ \iff \frac{1}{N} \mathbf{X}^T \mathbf{H} \mathbf{X} \mathbf{W} \mathbf{W}^T \mathbf{X}^T \mathbf{H} \mathbf{X} \mathbf{W} &= \mathbf{X}^T \left(\mathbf{H} - \frac{\gamma}{\alpha} \mathbf{L} \right) \mathbf{X} \mathbf{W} \\ \iff \mathbf{W} \mathbf{W}^T \text{Cov}(\mathbf{X}) \mathbf{W} &= \frac{1}{N} \text{Cov}(\mathbf{X})^{-1} \mathbf{X}^T \left(\mathbf{H} - \frac{\gamma}{\alpha} \mathbf{L} \right) \mathbf{X} \mathbf{W}, \end{aligned}$$

denoting for clarity $\mathbf{A} \triangleq \text{Cov}(\mathbf{X})$ and $\mathbf{B} \triangleq \frac{1}{N} \mathbf{X}^T \left(\mathbf{H} - \frac{\gamma}{\alpha} \mathbf{L} \right) \mathbf{X} = \text{Cov}(\mathbf{X})^{-1} - \frac{\gamma}{\alpha} \mathbf{X}^T \mathbf{L} \mathbf{X}$ we have

$$\mathbf{W} \mathbf{W}^T \mathbf{A} \mathbf{W} = \mathbf{A}^{-1} \mathbf{B} \mathbf{W},$$

which is solved for $\mathbf{W} = \mathbf{A}^{-1} \sqrt{\mathbf{B}}$. Now, if $K < D$ then there are multiple local minimum, all with the same loss value, and those are obtained by extracting any K -out-of- D columns of the above solution. For Eq. (12) we considered the first K columns arbitrarily.

A.10 Proof of Laplacian estimation with contrastive learning Theorem 4

The first step of the proof consists in recovering the softmax with any metric d that computes the distance (whatever distance desired) between pairs of inputs.

Graph Laplacian Estimation recovers the step 1 of contrastive methods using \mathcal{R}_{\log} . To prove Eq. (16) (the case with \mathcal{G} and not $\mathcal{G}_{\text{rsto}}$ can be done similarly by removing the row-sum-to-one constraint), we need to solve the following optimization problem

$$\arg \min_{\mathbf{W} \in \mathcal{G}_{\text{rsto}}} \sum_{i \neq j} d(f_{\theta}(\mathbf{x}_i), f_{\theta}(\mathbf{x}_j)) \mathbf{W}_{i,j} + \tau \sum_{i \neq j} \mathbf{W}_{i,j} (\log(\mathbf{W}_{i,j}) - 1),$$

which we solve by introducing the constraint in the optimization problem with the Lagrangian to

$$\begin{aligned} \mathcal{L} &= \sum_{i \neq j} d(f_{\theta}(\mathbf{x}_i), f_{\theta}(\mathbf{x}_j)) \mathbf{W}_{i,j} + \tau \sum_{i \neq j} \mathbf{W}_{i,j} (\log(\mathbf{W}_{i,j}) - 1) + \sum_{i=1}^N \lambda_i (\sum_{j \neq i} \mathbf{W}_{i,j} - 1) + \sum_i \beta_i \mathbf{W}_{i,i} \\ \implies \frac{\partial \mathcal{L}}{\partial \mathbf{W}_{i,j}} &= \begin{cases} d(f_{\theta}(\mathbf{x}_i), f_{\theta}(\mathbf{x}_j)) + \tau \log(\mathbf{W}_{i,j}) + \lambda_i & \iff i \neq j \\ \beta_i & \iff i = j \end{cases} \\ \implies \frac{\partial \mathcal{L}}{\partial \lambda_i} &= \sum_{j \neq i} \mathbf{W}_{i,j} - 1 \\ \implies \frac{\partial \mathcal{L}}{\partial \beta_i} &= \mathbf{W}_{i,i}, \end{aligned}$$

we first solve for $\frac{\partial \mathcal{L}}{\partial \mathbf{W}_{i,j}} = 0$ for $i \neq j$ to obtain an expression of $\mathbf{W}_{i,j}$ as a function of λ_i as

$$\begin{aligned} \frac{\partial \mathcal{L}}{\partial \mathbf{W}_{i,j}} = 0 &\iff d(f_{\theta}(\mathbf{x}_i), f_{\theta}(\mathbf{x}_j)) + \tau \log(\mathbf{W}_{i,j}) + \lambda_i = 0 \\ &\iff \tau \log(\mathbf{W}_{i,j}) = -d(f_{\theta}(\mathbf{x}_i), f_{\theta}(\mathbf{x}_j)) - \lambda_i \\ &\iff \mathbf{W}_{i,j} = e^{\frac{-1}{\tau}(d(f_{\theta}(\mathbf{x}_i), f_{\theta}(\mathbf{x}_j)) + \lambda_i)} \\ &\iff \mathbf{W}_{i,j} = e^{\frac{-1}{\tau}d(f_{\theta}(\mathbf{x}_i), f_{\theta}(\mathbf{x}_j))} e^{\frac{-1}{\tau}\lambda_i}, \end{aligned}$$

and now using $\frac{\partial \mathcal{L}}{\partial \lambda_i} = 0$ we will be able to solve for λ_i as follows

$$\begin{aligned} \frac{\partial \mathcal{L}}{\partial \lambda_i} = 0 &\iff \sum_{j \neq i} \mathbf{W}_{i,j} - 1 = 0 \\ &\iff e^{\frac{-\lambda_i}{\tau}} \sum_{j \neq i} e^{\frac{-1}{\tau}d(f_{\theta}(\mathbf{x}_i), f_{\theta}(\mathbf{x}_j))} = 1 \\ &\iff e^{\frac{-\lambda_i}{\tau}} = \frac{1}{\sum_{j \neq i} e^{\frac{-1}{\tau}d(f_{\theta}(\mathbf{x}_i), f_{\theta}(\mathbf{x}_j))}}, \end{aligned}$$

which allows us to finally obtain an explicit solution for $\frac{\partial \mathcal{L}}{\partial \mathbf{W}_{i,j}} = 0$ that does not depend on λ_i as follows

$$\begin{aligned} \frac{\partial \mathcal{L}}{\partial \mathbf{W}_{i,j}} = 0 &\iff \mathbf{W}_{i,j} = e^{\frac{-1}{\tau}d(f_{\theta}(\mathbf{x}_i), f_{\theta}(\mathbf{x}_j))} e^{\frac{-\lambda_i}{\tau}} \\ &\iff \mathbf{W}_{i,j} = \frac{e^{\frac{-1}{\tau}d(f_{\theta}(\mathbf{x}_i), f_{\theta}(\mathbf{x}_j))}}{\sum_{j \neq i} e^{\frac{-1}{\tau}d(f_{\theta}(\mathbf{x}_i), f_{\theta}(\mathbf{x}_j))}} \end{aligned}$$

which holds for $i \neq j$. Now for the case $i = j$ simply using the constraint and solving for β_i directly gives $\mathbf{W}_{i,i} = 0$. Notice that we did not enforce the $\mathbf{W}_{i,j} = \mathbf{W}_{j,i}$ constraint, however, the optimum found fulfills it and thus we are in a scenario akin to undirected graph Laplacian estimation.

Recovering SimCLR with Cosine Similarity. Now, since we are using the cosine distance, defined as $f(\mathbf{x}, \mathbf{y}) = 1 - \frac{\langle \mathbf{x}, \mathbf{y} \rangle}{\|\mathbf{x}\| \|\mathbf{y}\|}$, we can plug it in the above to finally obtain

$$\mathbf{W}_{i,j} = \frac{e^{\frac{-1}{\tau}d(f_{\theta}(\mathbf{x}_i), f_{\theta}(\mathbf{x}_j))}}{\sum_{j \neq i} e^{\frac{-1}{\tau}d(f_{\theta}(\mathbf{x}_i), f_{\theta}(\mathbf{x}_j))}} \mathbf{1}_{\{i \neq j\}} = \frac{e^{\frac{1}{\tau} \frac{\langle f_{\theta}(\mathbf{x}_i), f_{\theta}(\mathbf{x}_j) \rangle}{\|f_{\theta}(\mathbf{x}_i)\|_2 \|f_{\theta}(\mathbf{x}_j)\|_2}}}{\sum_{j \neq i} e^{\frac{1}{\tau} \frac{\langle f_{\theta}(\mathbf{x}_i), f_{\theta}(\mathbf{x}_j) \rangle}{\|f_{\theta}(\mathbf{x}_i)\|_2 \|f_{\theta}(\mathbf{x}_j)\|_2}}} \mathbf{1}_{\{i \neq j\}},$$

which is exactly the features used by SimCLR or NNCLR. The last step is direct, take the graph of known positive pairs of nearest neighbor, apply the cross entropy between those and the above, and one obtains that Eq. (16) recovers exactly the loss of those models.

Graph Laplacian Estimation recovers the step 1 of contrastive methods using \mathcal{R}_F . We will be using the $\mathcal{G}_{\text{rsto}}$ space again as the case for \mathcal{G} can be obtained easily by removing the Lagrangian constraint. we need to solve the following optimization problem

$$\arg \min_{\mathbf{W} \in \mathcal{G}_{\text{rsto}}} \sum_{i \neq j} d(f_{\theta}(\mathbf{x}_i), f_{\theta}(\mathbf{x}_j)) \mathbf{W}_{i,j} + \tau \sum_{i \neq j} \mathbf{W}_{i,j} (\mathbf{W}_{i,j}/2 - 1),$$

which is augmented with the constraints to

$$\mathcal{L} = \sum_{i \neq j} d(f_{\theta}(\mathbf{x}_i), f_{\theta}(\mathbf{x}_j)) \mathbf{W}_{i,j} + \tau \sum_{i \neq j} \mathbf{W}_{i,j} (\mathbf{W}_{i,j}/2 - 1) + \sum_{i=1}^N \lambda_i (\sum_{j \neq i} \mathbf{W}_{i,j} - 1) + \sum_i \beta_i \mathbf{W}_{i,i}$$

which we will differentiate with respect to \mathbf{W} , λ , β to obtain given \mathcal{L} above

$$\begin{aligned} \Rightarrow \frac{\partial \mathcal{L}}{\partial \mathbf{W}_{i,j}} &= \begin{cases} d(f_{\theta}(\mathbf{x}_i), f_{\theta}(\mathbf{x}_j)) + \tau \mathbf{W}_{i,j} - \tau + \lambda_i & \Leftrightarrow i \neq j \\ \beta_i & \Leftrightarrow i = j \end{cases} \\ \Rightarrow \frac{\partial \mathcal{L}}{\partial \lambda_i} &= \sum_{j \neq i} \mathbf{W}_{i,j} - 1 \\ \Rightarrow \frac{\partial \mathcal{L}}{\partial \beta_i} &= \mathbf{W}_{i,i}, \end{aligned}$$

setting $\frac{\partial \mathcal{L}}{\partial \mathbf{W}_{i,j}}$ to 0 we will obtain the following simplification isolating λ_i for $i \neq j$

$$\begin{aligned} \frac{\partial \mathcal{L}}{\partial \mathbf{W}_{i,j}} = 0 &\Leftrightarrow d(f_{\theta}(\mathbf{x}_i), f_{\theta}(\mathbf{x}_j)) + \tau \mathbf{W}_{i,j} - \tau + \lambda_i = 0 \\ &\Leftrightarrow \mathbf{W}_{i,j} = 1 - \frac{1}{\tau} (d(f_{\theta}(\mathbf{x}_i), f_{\theta}(\mathbf{x}_j)) + \lambda_i) \end{aligned}$$

and now using $\frac{\partial \mathcal{L}}{\partial \lambda_i} = 0$ we will obtain

$$\begin{aligned} \frac{\partial \mathcal{L}}{\partial \lambda_i} = 0 &\Leftrightarrow \sum_{j \neq i} \mathbf{W}_{i,j} - 1 = 0 \\ &\Leftrightarrow \sum_{j \neq i} \left(1 - \frac{1}{\tau} (d(f_{\theta}(\mathbf{x}_i), f_{\theta}(\mathbf{x}_j)) + \lambda_i) \right) - 1 = 0 \\ &\Leftrightarrow N - 1 + \frac{-\sum_{j \neq i} d(f_{\theta}(\mathbf{x}_i), f_{\theta}(\mathbf{x}_j))}{\tau} - \frac{(N-1)\lambda_i}{\tau} - 1 = 0 \\ &\Leftrightarrow \lambda_i = \frac{-\sum_{j \neq i} d(f_{\theta}(\mathbf{x}_i), f_{\theta}(\mathbf{x}_j))}{(N-1)} + \tau \left(1 - \frac{1}{N-1} \right) \end{aligned}$$

and then plugging that into the original system of equation leads to

$$\begin{aligned} \frac{\partial \mathcal{L}}{\partial \mathbf{W}_{i,j}} = 0 &\Leftrightarrow \mathbf{W}_{i,j} = 1 - \frac{1}{\tau} (d(f_{\theta}(\mathbf{x}_i), f_{\theta}(\mathbf{x}_j)) + \lambda_i) \\ &\Leftrightarrow \mathbf{W}_{i,j} = 1 - \frac{1}{\tau} \left(d(f_{\theta}(\mathbf{x}_i), f_{\theta}(\mathbf{x}_j)) + \left(\frac{-\sum_{j \neq i} d(f_{\theta}(\mathbf{x}_i), f_{\theta}(\mathbf{x}_j))}{(N-1)} + \tau \left(1 - \frac{1}{N-1} \right) \right) \right) \\ &\Leftrightarrow \mathbf{W}_{i,j} = \frac{1}{N-1} - \frac{1}{\tau} \left(d(f_{\theta}(\mathbf{x}_i), f_{\theta}(\mathbf{x}_j)) - \frac{\sum_{j \neq i} d(f_{\theta}(\mathbf{x}_i), f_{\theta}(\mathbf{x}_j))}{(N-1)} \right) \end{aligned}$$

for any $i \neq j$. Again solving for β_i will lead directly to $\mathbf{W}_{i,i} = 0$. In matrix form, we thus obtain $\mathbf{W} = \frac{1}{N-1} (\mathbf{1}\mathbf{1}^T - \mathbf{I}) - \frac{1}{\tau} \left(\mathbf{D} - \frac{1}{N-1} \mathbf{D}\mathbf{1}\mathbf{1}^T \right)$ since the diagonal elements of \mathbf{D} are 0.

A.11 Proof of SimCLR Theorem 5

The goal of this section is to demonstrate that SimCLR, although optimizing the graph estimate $\widehat{\mathbf{G}}$ to match \mathbf{G} forces the representation \mathbf{Z} to match \mathbf{G} through its outer-product. This result closely follows a multidimensional scaling type of reasoning which should not be a surprise being a global spectral embedding method. Let's say that τ is for example 1 and that all distances are between 0 and 1 e.g. using the cosine distance to streamline the derivations (if not, simply set τ to the maximum value present in the matrix \mathbf{D}). We thus obtain

$$\|\mathbf{G} - \widehat{\mathbf{G}}\|_F^2 = \|(\mathbf{1}\mathbf{1}^T - \mathbf{I} - \mathbf{G}) - ((\mathbf{1}\mathbf{1}^T - \mathbf{I} - \widehat{\mathbf{G}}))\|_F^2 = \|\underbrace{(\mathbf{1}\mathbf{1}^T - \mathbf{I} - \mathbf{G}) + \mathbf{D}}_{\triangleq \mathbf{D}'}\|_F^2$$

and now we will basically decompose the loss into two orthogonal terms as follows using the centering matrix i.e. Householder transformation $\mathbf{H} = \mathbf{I} - \frac{1}{N}\mathbf{1}\mathbf{1}^T$ and noting that $\mathbf{H}\mathbf{1} = \mathbf{0}$. We simplify

$$\begin{aligned} \|\mathbf{D}' - \mathbf{D}\|_F^2 &= \left\| \left(\mathbf{H} + \frac{1}{N}\mathbf{1}\mathbf{1}^T \right) (\mathbf{D}' - \mathbf{D}) \left(\mathbf{H} + \frac{1}{N}\mathbf{1}\mathbf{1}^T \right) \right\|_F^2 \quad (\text{since } \mathbf{H} + \frac{1}{N}\mathbf{1}\mathbf{1}^T = \mathbf{I}) \\ &= \|\mathbf{H}(\mathbf{D}' - \mathbf{D})\mathbf{H}\|_F^2 + 2\text{Tr} \left(\mathbf{H}(\mathbf{D}' - \mathbf{D}) \frac{1}{N}\mathbf{1}\mathbf{1}^T \right) + \left\| \frac{1}{N}\mathbf{1}\mathbf{1}^T (\mathbf{D}' - \mathbf{D}) \frac{1}{N}\mathbf{1}\mathbf{1}^T \right\|_F^2 \\ &= \|\mathbf{H}(\mathbf{D}' - \mathbf{D})\mathbf{H}\|_F^2 + \left\| \frac{1}{N}\mathbf{1}\mathbf{1}^T (\mathbf{D}' - \mathbf{D}) \frac{1}{N}\mathbf{1}\mathbf{1}^T \right\|_F^2 \\ &= \|\mathbf{H}(\mathbf{D}' - \mathbf{D})\mathbf{H}\|_F^2 + (\text{mean}(\mathbf{D}) - \text{mean}(\mathbf{D}'))^2 \\ &= 4 \left\| -\frac{1}{2}\mathbf{H}\mathbf{D}'\mathbf{H} - \left(-\frac{1}{2}\mathbf{H}\mathbf{D}\mathbf{H}\right) \right\|_F^2 + (\text{mean}(\mathbf{D}) - \text{mean}(\mathbf{D}'))^2 \\ &= 4 \left\| -\frac{1}{2}\mathbf{H}\mathbf{D}'\mathbf{H} - \mathbf{H}\mathbf{Z}\mathbf{Z}^T\mathbf{H} \right\|_F^2 + (\text{mean}(\mathbf{D}) - \text{mean}(\mathbf{D}'))^2 \\ &= 4 \|\mathbf{H}(\mathbf{G} + \mathbf{I} - 2\mathbf{Z}\mathbf{Z}^T)\mathbf{H}\|_F^2 + (\text{mean}(\mathbf{D}) - \text{mean}(\mathbf{D}'))^2 \end{aligned}$$

which can then be minimized using [Higham, 1988] to obtain that \mathbf{Z} will be proportional to the first K eigenvectors of $\mathbf{G} + \mathbf{I}$ rescaled by the square root of their eigenvalues divided by 2τ . For the case with softmax and cross-entropy, we entirely leverage on Corollary 2.2 of Ganea et al. [2019] (a study done in the context of the softmax dimensional bottleneck [Yang et al., 2017]) where it was shown that the minimum of the cross entropy loss is obtained whenever the rank of the pre-activations (logits) of the true and predicted probabilities have same rank. As soon as one uses an ϵ label-smoothing, to ensure that the logits of the distribution (rows of \mathbf{G}) do not go to infinity in the case where a row contains only a single 1, we obtain the desired result. For the RBF case, it is proven to be always nonsingular, regardless of the value of the temperature parameter, as long as the samples are all distinct [Knaf, 2007], hence in our case, the only solution to minimize the loss is for the samples (features maps in this case) to collapse i.e. for the rank of \mathbf{Z} to align with the one of \mathbf{G} , see Wathen and Zhu [2015] for other kernels.

A.12 SimCLR/NNCLR recovers ISOMAP and MDS (Proposition 2)

This proof essentially follows the same derivations than Appendix A.11 up until the last equality. Then, one can see that the eigenvectors of \mathbf{G} and $\mathbf{G} + \mathbf{I}$ are identical (only the eigenvalues are shifted by 1). Hence, up to a rescaling, solving the ISOMAP optimization problem or the SimCLR one are equivalent, up to shift and rescaling of the representations.

A.13 Barlow Twins optimal Representation (Theorem 6)

Canonical correlation analysis usually takes the form of an optimization problem searching over linear weights \mathbf{W} that maximally correlates the transformed inputs. In our case, we ought to work directly with the representation as it is the final input representation that is being fed into the BarlowTwins loss. To ease this proof, we will heavily rely on the derivations from Appendix A.16 since it offers the exact link between BarlowTwins and Canonical Correlation Analysis. The kernel version is nothing more than linear CCA but with input the $\phi(\mathbf{x}_n)$ representations as opposed to the actual inputs \mathbf{x}_n . Hence Appendix A.16 can be used

in the same way to obtain that BarlowTwins with a nonlinear DN recovers Kernel CCA. Now, the key result concerns the rank of the representation. First, we ought to recall that we are working with the regularized version of CCA that adds a small constant to the denominator of the cosine similarity computation between the columns of \mathbf{Z}_a and \mathbf{Z}_b .

A.14 Linear VICReg is Locality Preserving Projection (Theorem 3)

For the following result, we will assume that $\mathbf{X}^T(\mathbf{D} - \mathbf{G})\mathbf{X}$ is invertible for clarity of notations, although not required for a solution to exist [Liang et al., 2013]. This assumption holds as long as the within-connected components (resp. within-class) variance of the samples is positive. Given that, it is well known that Laplacian Eigenmap with linear mapping of the input produces LPP, hence the proof essentially relies on Appendix A.8 that ties VICReg with Laplacian Eigenmap, and then e.g. on [Kokopoulou et al., 2011] for that known relationship between those two models.

A.15 Linear VICReg with supervised relation matrix is LDA (Theorem 3)

We should highlight that the exact LDA employs an optimization problem that is typically nonconvex, and for which there does not exist a closed-form solution [Webb, 2003]. Hence it is common to look at a simpler optimization problem instead [Guo et al., 2003, Wang et al., 2007] which is the one that VICReg closed-form solution recovers. For this section and without loss of generality we simplify our notations by assuming that \mathbf{G} as a degree matrix of \mathbf{I} i.e. the sum of each row sum to one. The objective in 2-class LDA (see Li and Wang [2014] for examples) is to minimize the following objective

$$\max_{\mathbf{w}} \frac{\mathbf{w}^T \boldsymbol{\Sigma}_b \mathbf{w}}{\mathbf{w}^T \boldsymbol{\Sigma}_w \mathbf{w}},$$

where $\boldsymbol{\Sigma}_t = \mathbf{X}^T \mathbf{X}$, $\boldsymbol{\Sigma}_w = \mathbf{X}^T (\mathbf{I} - \mathbf{G}) \mathbf{X}$, $\boldsymbol{\Sigma}_b = \mathbf{X}^T \mathbf{G} \mathbf{X}$ encode the total/within/between cluster variances respectively using the supervised relation matrix \mathbf{G} . In fact, (assuming for clarity that the inputs have 0 mean) one has

$$\begin{aligned} \frac{1}{N} \mathbf{X}^T \mathbf{G} \mathbf{X} &= \frac{1}{N} \sum_{c=1}^C \sum_{i \in \mathcal{N}_c} \sum_{j \in \mathcal{N}_c} \frac{1}{N_c} \mathbf{x}_i \mathbf{x}_j^T \\ &= \frac{1}{N} \sum_{c=1}^C N_c \sum_{i \in \mathcal{N}_c} \sum_{j \in \mathcal{N}_c} \frac{1}{N_c^2} \mathbf{x}_i \mathbf{x}_j^T \\ &= \frac{1}{N} \sum_{c=1}^C N_c \frac{\sum_{i \in \mathcal{N}_c} \mathbf{x}_i}{N_c} \frac{\sum_{j \in \mathcal{N}_c} \mathbf{x}_j^T}{N_c} \\ &= \sum_{c=1}^C \frac{N_c}{N} \boldsymbol{\mu}_c \boldsymbol{\mu}_c^T, \end{aligned}$$

recovering the between (inter-cluster) variance $\boldsymbol{\Sigma}_b$ with $\boldsymbol{\mu}_c$ the center of class c . Now, since we have that $\boldsymbol{\Sigma}_t = \boldsymbol{\Sigma}_b + \boldsymbol{\Sigma}_w$ we directly have that $\boldsymbol{\Sigma}_w = \frac{1}{N} (\mathbf{X}^T \mathbf{X} - \mathbf{X}^T \mathbf{G} \mathbf{X}) = \frac{1}{N} (\mathbf{X}^T (\mathbf{I} - \mathbf{G}) \mathbf{X})$. Given that, one can directly solve the LDA problem (in this case we provide directly the multivariate setting) via

$$\max_{\mathbf{W}} \frac{|\mathbf{W}^T \boldsymbol{\Sigma}_b \mathbf{W}|}{|\mathbf{W}^T \boldsymbol{\Sigma}_w \mathbf{W}|},$$

which is known as the Fisher criterion. Whenever $\boldsymbol{\Sigma}_w$ is invertible (if not, then the original data can be projected to a lower dimensional subspace without loss on information that would ensure that $\boldsymbol{\Sigma}_w$ is invertible) then Fisher's criterion is maximized leading to \mathbf{W} being the solution to the generalized eigenvalue problem

$$\mathbf{W}^* = \arg \max_{\mathbf{W}} \frac{|\mathbf{W}^T \boldsymbol{\Sigma}_b \mathbf{W}|}{|\mathbf{W}^T \boldsymbol{\Sigma}_w \mathbf{W}|} = \text{top eigenvectors of: } (\boldsymbol{\Sigma}_w)^{-1} \boldsymbol{\Sigma}_b.$$

Notice that the generalized eigenvalue problem is exactly

$$\mathbf{X}^T \mathbf{G} \mathbf{X} \mathbf{W} = \text{diag}(\lambda) \mathbf{X}^T (\mathbf{I} - \mathbf{G}) \mathbf{X} \mathbf{W},$$

and that $G\mathbf{1} = \mathbf{1}$ we observe that this is exactly the same solution than the LPP problem with G being the relation matrix and I being the degree matrix of the graph. Hence we obtain that LPP is equivalent to LDA whenever one uses the supervised relation matrix G as G (which was first pointed out in Kokopoulou et al. [2011]) and that it corresponds exactly to VICReg in the linear regime (as per Appendix A.14). We also note that the eigenvalue of the above matrix $(\Sigma_w)^{-1}\Sigma_b$ might seem to be arbitrary. However we have the following lemma that ensure that the eigenvalues of are real nonnegative.

Lemma 1. *The eigenvalues of $(\Sigma_w)^{-1}\Sigma_b$ are equal to the eigenvalues of $\Sigma_w^{-1/2}\Sigma_b\Sigma_w^{-1/2}$ which is symmetric hence all are nonnegative and real.*

A.16 Proof of BarlowTwins in the Linear Regime (Theorem 7)

The tie between CCA and LDA is not new. In fact, if one considers one dataset to be the samples and the other to be the class labels (binary variables for two-class problems or a variation of one-hot encoding for multi-class problems) then CCA and LDA are equivalent [Bartlett, 1938, Hastie et al., 1995]. But in our case, we do not explicitly use the labels but the views of different class. Hence, the goal of this section is to first recover the analytical parameters of BarlowTwins in the linear regime through CCA and then to demonstrate that the CCA-LDA connection also persists in the case when the views are both obtained from per-class samples i.e. exactly fitting the BarlowTwins scenario.

There exists many different ways to formulate the CCA problem. At the most simple level, one aims to sequentially learn pairs of filters that produce maximally correlated features as in

$$\max_{\mathbf{w}_a, \mathbf{w}_b} \frac{\langle \mathbf{X}_a \mathbf{W}_a, \mathbf{X}_b \mathbf{W}_b \rangle}{\|\mathbf{X}_a \mathbf{W}_a\|_2 \|\mathbf{X}_b \mathbf{W}_b\|_2},$$

which can easily be recognized to be the diagonal element of the BarlowTwins loss that we aim to maximize in the linear regime i.e. the cosine similarity between a column of \mathbf{Z}_a and the same column of \mathbf{Z}_b . To find the corresponding filters, which are in general not assume to be identical, one transforms the above problem to a constrained optimization problem exactly as done with eigenvalue problems with the Rayleigh quotient. We thus obtain the following

$$\max_{\mathbf{w}_a, \mathbf{w}_b} \langle \mathbf{X}_a \mathbf{W}_a, \mathbf{X}_b \mathbf{W}_b \rangle \text{ s.t. } \|\mathbf{X}_a \mathbf{W}_a\|_2 = 1 \text{ and } \|\mathbf{X}_b \mathbf{W}_b\|_2 = 1,$$

since rescaling of the weights does not impact the learned filters, which can be transformed into a Lagrangian function as

$$\mathcal{L} = \langle \mathbf{X}_a \mathbf{W}_a, \mathbf{X}_b \mathbf{W}_b \rangle - \lambda_1 (\|\mathbf{X}_a \mathbf{W}_a\|_2 - 1) - \lambda_2 (\|\mathbf{X}_b \mathbf{W}_b\|_2 - 1),$$

which has the following partial derivatives using the Σ_{ab} notations for the cross-products

$$\begin{aligned} \nabla_{\mathbf{w}_a} \mathcal{L} &= \Sigma_{ab} \mathbf{w}_b - 2\lambda_1 \Sigma_{aa} \mathbf{w}_a \\ \nabla_{\mathbf{w}_b} \mathcal{L} &= \Sigma_{ba} \mathbf{w}_a - 2\lambda_2 \Sigma_{bb} \mathbf{w}_b \\ \frac{\partial \mathcal{L}}{\partial \lambda_1} &= \mathbf{w}_a^T \Sigma_{aa} \mathbf{w}_a \\ \frac{\partial \mathcal{L}}{\partial \lambda_2} &= \mathbf{w}_b^T \Sigma_{bb} \mathbf{w}_b, \end{aligned}$$

the first thing to notice is that setting those (first two) to zero will lead to $\lambda_1 = \lambda_2$ which we thus denote as a single λ parameter since

$$\begin{aligned} \Sigma_{ab} \mathbf{w}_b - 2\lambda_1 \Sigma_{aa} \mathbf{w}_a = 0 &\implies \mathbf{w}_a^T \Sigma_{ab} \mathbf{w}_b - 2\lambda_1 \mathbf{w}_a^T \Sigma_{aa} \mathbf{w}_a = 0 \implies \lambda_1 = \frac{1}{2} \mathbf{w}_a^T \Sigma_{ab} \mathbf{w}_b \\ \Sigma_{ba} \mathbf{w}_a - 2\lambda_2 \Sigma_{bb} \mathbf{w}_b = 0 &\implies \mathbf{w}_b^T \Sigma_{ba} \mathbf{w}_a - 2\lambda_2 \mathbf{w}_b^T \Sigma_{bb} \mathbf{w}_b = 0 \implies \lambda_2 = \frac{1}{2} \mathbf{w}_b^T \Sigma_{ba} \mathbf{w}_a, \end{aligned}$$

and thus we can simplify the original system using a single Lagrangian multiplier to have the following system

$$\left. \begin{aligned} \Sigma_{ab} \mathbf{w}_b - 2\lambda \Sigma_{aa} \mathbf{w}_a &= 0 \\ \Sigma_{ba} \mathbf{w}_a - 2\lambda \Sigma_{bb} \mathbf{w}_b &= 0 \end{aligned} \right\} \left(\frac{1}{4} \Sigma_{bb}^{-1} \Sigma_{ba} \Sigma_{aa}^{-1} \Sigma_{ab} - \lambda^2 \mathbf{I} \right) \mathbf{w}_b = \mathbf{0} \left. \begin{aligned} \mathbf{w}_a &= \frac{1}{2\lambda} \Sigma_{aa}^{-1} \Sigma_{ab} \mathbf{w}_b \end{aligned} \right\},$$

where it is clear that one obtains \mathbf{w}_b by solving the generalized eigenvalue problem and then finds \mathbf{w}_a accordingly and this can be done by remove the $\frac{1}{4}$ factor and replacing 2λ by λ . For specific implementations of the above, we direct the reader to Healy [1957], Ewerbring and Luk [1989], Hardoon et al. [2004].

Recovering LDA from supervised CCA. To recover this result, we closely follow the methodology from Kursun et al. [2011]. Additionally, we obtain that in this case the two views are permutation of each other due to the symmetric structure of \mathbf{G} that simply shuffles around the (repeated) samples to consider all the within-class pairs. Recall that even in this case \mathbf{G} as for degree matrix \mathbf{I} since we only use positive pairs between the samples (the dataset has been augmented first duplicating each input in each class to match with all others). In that setting, we first have the following simplifications We obtain

$$\Sigma_{aa} = \mathbf{Z}^T \mathbf{Z}, \quad \Sigma_{ab} = \mathbf{Z}^T \mathbf{G} \mathbf{Z}, \quad \Sigma_{ba} = \mathbf{Z}^T \mathbf{G} \mathbf{Z}, \quad \Sigma_{bb} = \mathbf{Z}^T \mathbf{Z},$$

since we have that $\mathbf{G} = \mathbf{G}^T$ and $\mathbf{G}^2 = \mathbf{I}$. Using the result from CCA Uurtio et al. [2017] we have the the CCA is equal to the sum of the singular values of $\Sigma_{bb}^{-1} \Sigma_{ba} C_{aa}^{-1} \Sigma_{ab}$ which corresponds to $\text{Tr}((\mathbf{Z}^T \mathbf{Z})^{-1} \mathbf{Z}^T \mathbf{G} \mathbf{Z})$ since $\Sigma_{ab} = \Sigma_{ba}$ and $\Sigma_{aa} = \Sigma_{bb}$. First, notice that the CCA optimum solves the following eigenvalue problem

$$\Sigma_{aa}^{-1} \Sigma_{ab} \Sigma_{bb}^{-1} \Sigma_{ba} \mathbf{u}_{CCA} = \lambda_{CCA} \mathbf{u}_{CCA},$$

but noticing that in our case \mathbf{X}_1 and \mathbf{X}_t are permutations of each other, we directly obtain that

$$\Sigma_{aa}^{-1} \Sigma_{ab} \Sigma_{bb}^{-1} \Sigma_{ba} \mathbf{u}_{CCA} = \lambda_{CCA} \mathbf{u}_{CCA} \iff \Sigma_t^{-1} \Sigma_b \Sigma_t^{-1} \Sigma_b \mathbf{u}_{CCA} = \lambda_{CCA} \mathbf{u}_{CCA},$$

using the total, between and within-class covariance matrices. Now, starting from the LDA loss, we will see that we recover the CCA one thanks to the above facts

$$\begin{aligned} \Sigma_b \mathbf{u}_{LDA} &= \lambda_{LDA} \Sigma_w \mathbf{u}_{LDA} && \text{(original LDA parameter)} \\ \iff \Sigma_b \mathbf{u}_{LDA} &= \lambda_{LDA} (\Sigma_t - \Sigma_b) \mathbf{u}_{LDA} \\ \iff \Sigma_b (1 + \lambda_{LDA}) \mathbf{u}_{LDA} &= \lambda_{LDA} \Sigma_t \mathbf{u}_{LDA} \\ \iff \Sigma_b \mathbf{u}_{LDA} &= \frac{\lambda_{LDA}}{(1 + \lambda_{LDA})} \Sigma_t \mathbf{u}_{LDA} \\ \iff \Sigma_t^{-1} \Sigma_b \mathbf{u}_{LDA} &= \frac{\lambda_{LDA}}{(1 + \lambda_{LDA})} \mathbf{u}_{LDA} \\ \iff \Sigma_t^{-1} \Sigma_b \Sigma_t^{-1} \Sigma_b \mathbf{u}_{LDA} &= \left(\frac{\lambda_{LDA}}{1 + \lambda_{LDA}} \right)^2 \mathbf{u}_{LDA} && \text{(original CCA problem)} \end{aligned}$$

hence given the LDA or CCA solutions one can recover the others, the only difference lies in the singular values, which can also be found from each other. Also, recall that the eigenvalues are real positive as per lemma 1 ensuring the well posed division used above.

A.17 Proof of VICReg Optimality (Theorem 9)

The proof first uses Theorem 1 that demonstrates how the optimal representation \mathbf{Z} will have the left singular vectors of \mathbf{G} up to rotations for the ones with multiplicity greater than one. Then, using that, we obtain from Theorem 9 that if those singular vectors are able to span the left singular vectors of \mathbf{Y} then there exists a linear probe that will solve the task at hand, giving the desired result.